DESIGN AND DEVELOPMENT OF FRACTAL APERTURE COUPLED MICROSTSRIP PATCH ANTENNA FOR WIRELESS APPLICATIONS

A Dissertation Submitted in Partial Fulfillment of the Requirement for the Award of the Degree of

MASTER OF ENGINEERING

in

Wireless Communications

Submitted By

NAVNEET KAUR

Roll No. 801563015

Under Supervision of

Dr. Amanpreet Kaur

Assistant Professor, ECED

ELECTRONICS AND COMMUNICATION ENGINEERING DEPARTMENT

THAPAR UNIVERSITY, PATIALA, PUNJAB

JUNE, 2017

DECLARATION

I, Navneet Kaur hereby declare that the work presented in this thesis entitled "Design and Development of Fractal Aperture Coupled Microstsrip Patch Antenna for Wireless Applications" in fulfillment of the requirement for the award of degree of Master of Engineering submitted at Electronics and Communication Engineering department, Thapar University, Patiala is an authentic record of work carried out under supervision of Dr. Amanpreet Kaur (Assistant Professor, ECED) from 2016 to 2017. The matter presented in this has not been submitted either in part or full to any other university or institute for the award of any other degree.

Navneet

Date: 15-07-2017

(Navneet Kaur)

(801563015)

It is certified that the above statement made by the candidate is correct to the best of my knowledge and belief.

Amanpreet Kaur

Date: 15/7/17

(Dr. Amanpreet Kaur)

(Assistant Professor, ECED)

ACKNOWLEDGEMENT

It is my proud privilege to acknowledge and extend my gratitude to several people who helped me directly or indirectly in completion of this report. I express my heart full indebtedness and owe a deep sense of gratitude to my teacher and my faculty guides **Dr. Amanpreet Kaur** for their sincere guidance and support with encouragement to go ahead.

I am also thankful to **Dr. Alpana Agarwal**, Professor and Head, ECED, for providing us with the adequate infrastructure for carrying out the work. I am also thankful to **Dr. Hemdutt Joshi,** Associate Professor & P.G. Coordinator, ECED, for the motivation and inspiration and that triggered me for the work.

I would also like to thank my entire friends who have more or less contributed to the preparation of this report. Last but not the least, I would like to thank my parents for their years of unyielding love and encourage. They have always wanted the best for me and I admire their determination and sacrifice. The study has indeed helped me to explore knowledge and avenues related to my topic and I am sure it will help me in my future.

Navneet Kaur

801563015

ABSTRACT

The wireless industry has undergone a volatile emergence today in present era. Antenna the most important component of wireless system demand versatility and unobtrusiveness. Need of multiband antennas are increasing day by day due to need of covering maxinum applications. Fractal plays a prominent role for these requirements. Fractals have non-integral dimensions and their space filling capability could be used for miniaturing antenna size and their properties of self similarity in the geometry leads to have antennas which has more number of resonant frequencies. Fractal geometries when applied to UWB generator patch, improves gain, return loss and radiation characteristics. Often fractal antennas does not require any matching components to achieve multiband or broadband performance. Thus the research work presented here in thesis focuses on the design and simulation of a plus shped carpet fractal antenna, koch aperture coupled fractal antenna, complementary bowtie aperture coupled antenna and a cup shaped microstrip line fed antenna using CST(Computer Simulation software) microwave studio version 2014. The antennas are fed using aperture coupled feeding mechanism because it provides reasonably higher bandwidth as compared to other feeds and a moderate amount of spurious radiations A plus shaped carpet fractal antenna covers the frequency band ranging from 3.9-4.08 GHz, 4.8-5.06 GHz, 6.1-6.4 GHz, 6.93-11.39 GHz with adequate bandwidth of 180 MHz, 260 MHz, 300 MHz and 4460 MHz respectively. Koch fractal aperture coupled antenna covers the frequency band ranging from 5.3-9.2 GHz with adequate bandwidth of 3900 MHz resonating at 6.9 GHz, 8.0 GHz and 8.4 GHz respectively. Complementary bowtie antenna covers frequency range from 4.08-6.2 GHz with impedance bandwidth of 2120 MHz. A cup shaped fractal antenna covers the frequency range from 4.9-25.9 GHz with bandwidth of 21 GHz. In order to verify the antenna application in the practical scenario, plus shaped carpet fractal and bowtie aperture coupled antennas are fabricated using photolithography process and tested on a VNA and measured results are quite matching with simulated ones allowing the antenna to be suitable for WLAN, WiMAX, WIBAN, HIPERLAN, UWB, radio communication, satellite communication, radar communication applications.

TABLE OF CONTENTS

LISTS OF FIGURES

LISTS OF TABLES

LIST OF ABBREVIATIONS

CST MWS V14.0	*Computer Simulation Tool Microwave Studio Version 2014*
DGS	*Defected Ground Structure*
MSA	*Microstrip Antenna*
MPA	*Microstrsip Patch Antenna*
RADAR	*Radio Detection And Raining*
UWB	*Ultra wideband*
VNA	*Vector Network Analysis*
VSWR	*Voltage Standing Wave Ratio*
WiMAX	*Worldwide Interoperability for Microwave Access*
WLAN	*Wireless Local Area Network*

CHAPTER-1
INTRODUCTION

1.1 FRACTAL ANTENNAS

Antenna is the key element in for any wireless communication system. Antennas with multiband and low profile characteristics are in growing demand for commercial and military applications in any wireless communication system [1]. To meet the modern wireless standards and device necessities, antenna miniaturing is an another challenging demand [2]. Fractal geometries for this purpose with various antenna configurations and designs have been developed in recent research works. These low profile antennas are easily employable at multi-frequency band and preferred as multi-functional antennas [3].

As multiband operating antennas are also one of the foremost requirements in today's research field. Fractal antennas are aimed to be one of the solutions for obtaining these characteristics [4]. Fractal structures are preferred because of their compact size and self-similarity geometry which helps in achieving the desired results [5, 6]. The self-similar nature provides similar surface current distributions for various resonating frequencies. Additionally the space filling property of fractal antenna increases the electrical length of the radiating element. Further leaned size can be obtained at the desired resonate frequency. Fractal antennas with self-similarity property offer the same multiband behavior as that of conventional microstrip patch antenna (MPA) for accomplishing multi band behavior by using multiple radiating elements or relatively loaded patch antennas[7].

Fractals were studied by researchers a long back. In 1975, Benoit Mandelbrot characterized fractals for classifying structures whose measurements were not whole number. The rough terrain, ruggedness of coastline, branching of tree leaves and plants and numerous more such illustrations are utilized to characterize such structures. These structures cover different applications in the field of image compression and analysis of lightning phenomena at high elevations. They have unique characteristics that are associated to various geometries and properties of fractal [9-15].

Figure 1.1(a-c) shows that many natural object exhibit the fractal geometry eg. tree leaves, romanesco broccoli, coastline. This property of self similarity of fractals was successfully employed by scientists to develop fractal antennas that could yield a multiband/broadband behavior from a smaller antenna [9].

(a)

(b)

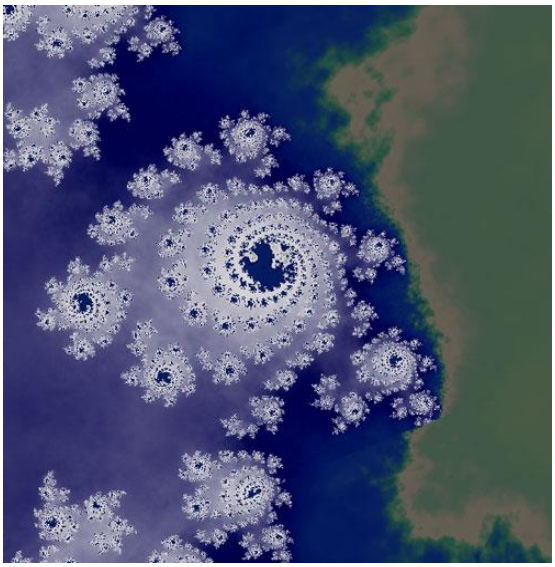

(c)

Figure 1.1 Photograph of (a) The Tree Patterns (b) broccoli (c) Coastline Developed using Fractals [9-15].

1.2 PROPERTIES OF FRACTAL ANTENNAS

Fractal antennas represent some unique properties which are discussed below

- Fractals exhibit self-similarity property. This is accomplished by carrying out various iterations at different scaling factor. Thus ease in designing.
- Space-filling is another unique property of fractals which results in the reduction of overall size of the antenna.
- Fractal antennas exhibit multiband behavior utilizing an iterative process which makes the antenna to radiate at more than one frequency.
- As compared to ordinary antenna, fractal antennas resonate at lower frequencies with smaller physical size which results in antenna miniaturization.

- These antennas are low profile and its fabrication cost is less.
- These antennas are robust against heat or mechanical strain.
- Provide much flexibility in designing and fabrication of the antenna.

Fractal antennas are responsible of multiband characteristics. These fractal geometries have numerous advantages when compared with conventional antennas. As microstrip antennas (MSA) have reduced structures and fractal geometries with above discussed features, antennas turn out to be more adaptable [16]. Fractals geometries incorporated with MSA have many advantages which are discussed in the following segment.

1.3 PREFERENCE OF MICROSTRIP PATCH ANTENNA FOR FRACTAL GEOMETRY

MPAs have many advantages when contrasted with conventional antennas [16]. They have discovered utilization in a wide variety of application such as embedded antenna in cellular phones, pagers etc and communication antennas on rockets and antennas in satellite communication. Some of their essential preferences are:

- They are light in weight and thus have small volume.
- They can be used in low profile planar configurations.
- Can be manufactured in large quantities because of its low fabrication cost.
- It supports both linear as well as circular polarization.
- Versatile and flexible in terms of electromagnetic characteristics.
- These antennas can be composed with variable frequencies and other characteristics using adaptive elements.
- These antennas are thin planar structures with compact sizes.

A lot of research work is available that concentrates on design of fractal MSA for wireless applications.

1.4 MICROSTRIP PATCH ANTENNAS

MPAs are widely recognized type of printed antennas. Their low profile, geometry and low cost are the significant features [16]. MPA has two parallel conductor separated by a thin dielectric substrate. In this layered structure the upper conductor is radiating element known as patch where as the lower conductor is considered as ground plane. In brief a dielectric substrate has radiating element on its one side with ground plane on the other as represented below:

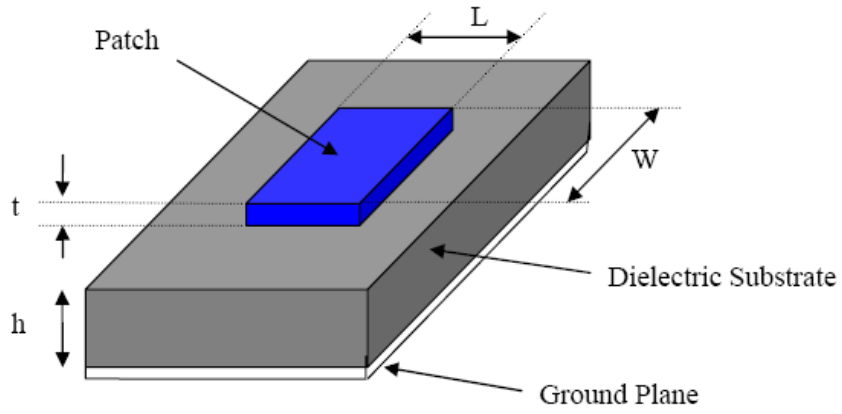

Figure 1.2 Microstrip Patch Antenna [16].

A copper or gold can be used as a conducting material for patch and is presented in many shapes. Few such patch shapes are represented below:

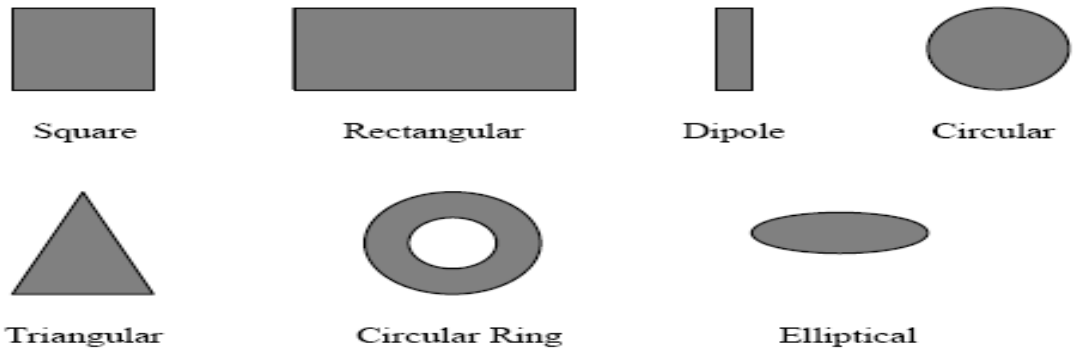

Figure 1.3 Different shapes of MPA [7].

The patch and feedline are photoetched on dielectric substrate. The radition of MPA is due to fringing field effect presented between patch and ground plane. The quality factor (Q) represents losses that are related to antennas and MPAs have high Q which include radiations, conduction dielectric and surface wave losses. Thin substrates have low surface wave losses and can be ignored where as for increased thickness, fraction of total power conveyed by source which goes into surface wave increases [17]. This surface wave degrades antenna performance as it contributes to undesirable power loss that ultimately scattered at dielectric bends. Thus to overcome this problem photonic band gap structures can be used. Other issues such as lower gain, less antenna efficiency, lower power handling capacity can be limited by utilizing antenna array arrangement.

1.5 FRACTAL GEOMETRY

In recent years many innovative designs of fractal geometries have been developed [9-15]. Some of them are shown below:

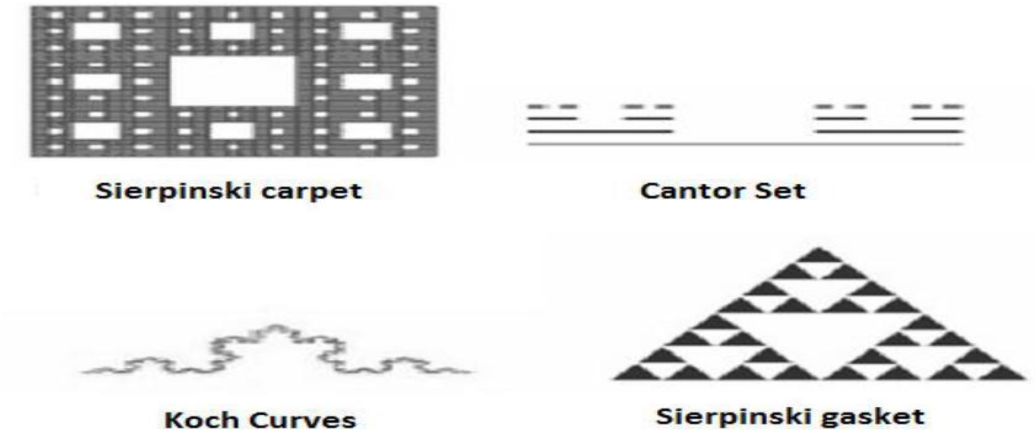

Figure 1.4 Types of Fractal Geometries [9-15].

The design of any type of fractal design is achieved using two main steps:

1. Initiator(0^{th} stage)
2. Generator

Initiator is the base state of the antenna geometry. From the area of initiator generator each subsequent iteration stage is added or subtracted thus resulting in the fractal structure. The design procedure of some common fractal geometries is mentioned in the next section.

1.6 TYPES OF FRACTAL GEOMETRIES

1.6.1 Sierpinski Gasket

The one such fractal geometry which is widely studied for various antenna applications is Sierpinski gasket geometry [17-23]. The steps followed for constructing such geometry is shown in Figure 1.5.

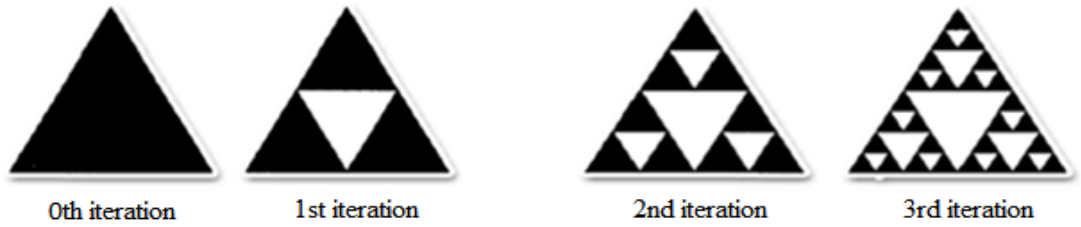

Figure 1.5 Steps of Construction for Gasket Geometry [10].

A triangle as an initiator is considered for 0^{th} iteration. 1^{st} iteration is carried out by embedding a triangular slot at midpoint of the sides of initiator triangle as shown in Figure 1.5. Similarly the procedure is repeated for rest of the iterations such that at each iteration the size of triangular slot is scaled as compared to the previous iteration. Sierpinski gasket fractal is constructed by performing this iterative process various times till the desired impedance bandwidth of antenna is achieved. In Figure 1.5, the dark triangular regions present the metal part whereas the grey part presents the area removed from metal. The design equation for design of Gasket is given in [11]. These equations include effective side length and effective length of the patch.

$$f_r = \begin{cases} (.15345 + .34\rho x)\left(\frac{c}{h_e}\right)(\xi^{-1}) for\ n = 0 \\ .26\left(\frac{c}{h_e}\right)\delta^n \qquad\qquad for\ n \neq 0 \end{cases}$$ Equation (1.1)

Where $\xi = \frac{h_k}{h_{k+1}}$ represents the ratio of height of triangle at K[th] iteration and k+1[th] iteration and $\delta = \frac{1}{\xi}$ represents scale factor.

1.6.2 Sierpinski Carpet

The procedure for construction of sierpinski carpet is same as that of sierpinski gasket, yet dissimilar to gasket, as it utilizes rectangles or square rather than triangles [24]. To begin with this kind of geometry, a generator is considered for 0[th] iteration as shown in Figure 1.6. Next iteration includes 9 sub-areas of equal size around centre patch and a square slot is placed at centre of each sub-area with length three times smaller than initial central patch.

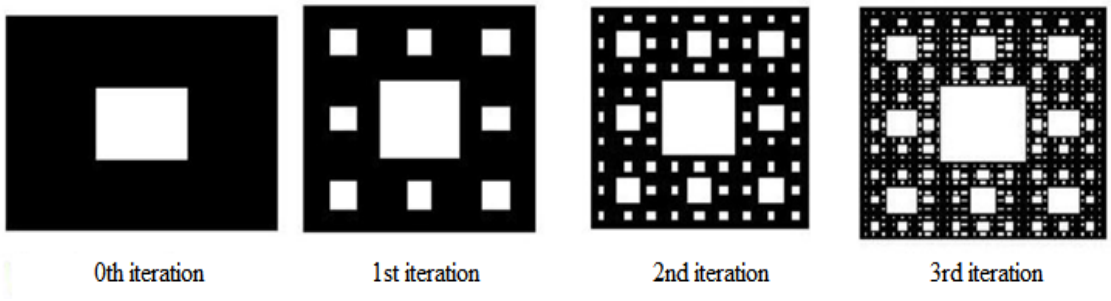

Figure 1.6 Sierpinski Carpet Geometry for Various Iterations [12].

All the square sizes are calculated using transmission line equations and the antenna is iterated till it gets optimized for desired results.

1.6.3 Koch Curve

The basic geometry of Koch curve is obtained by replacing the sides of equilateral triangle by a Koch curve. Triangle is considered as a generator for 0[th] iteration. For 1[st] iteration, a triangle of same side length as that of generator is placed with its vertices on opposite sides of initial triangle [25-31]. The procedure is utilized again in the era of higher iterations. The design equations (1.1) are utilized for planning Koch snowflake geometry.

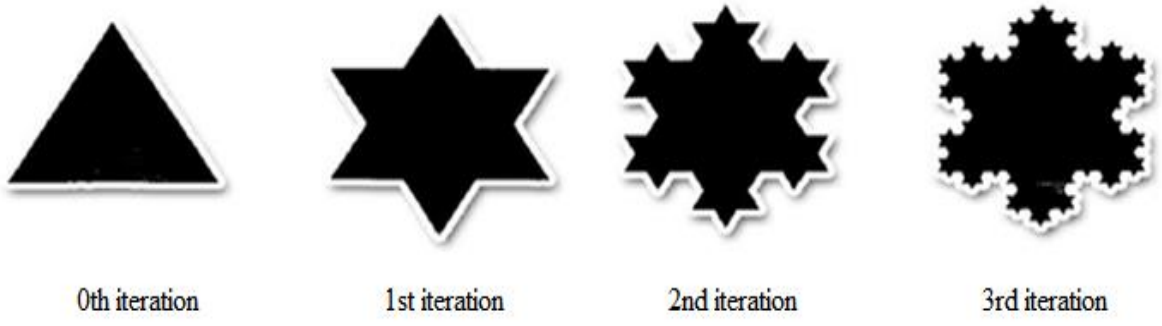

Figure 1.7 Steps of Construction for Koch Snowflake Geometry [13].

1.6.4 Hilbert Curve

Hilbert curve is another structure of the fractal family. Hilbert curve is created by four small duplicates of the generator however these duplicates are joined by extra line segments [14]. This geometry appears to be space-filling due to packing of more antennas in small volume. This geometry is self-avoiding no two segments intersect each other. If number of iterations increases then antenna can resonate at lower frequencies due to large electrical length when contrasted with the physical length. The length of each segment, total length of segment and resonant frequency is given by the formula represented below:

$$d = L/(2^n - 1) \qquad \text{Equation (1.2)}$$

$$s(n) = (L^{2n} - 1) * L/(2^n - 1) \qquad \text{Equation (1.3)}$$

$$\left(\frac{\mu_o}{\pi}\right) * k * \frac{\lambda}{4\left[log\left(\frac{8k\lambda}{b4}\right)-1\right]} = m * \frac{120}{w} * log\frac{2d}{b}\tan\beta d + \left(\frac{\mu_o}{\pi}\right)\left[\log\frac{8s}{b} - 1\right] \qquad \text{Equation (1.4)}$$

where L is the outer dimension, n is the fractal iteration, $m=4^{n-1}$ represents the length of parallel wire connection, b and k represents the diameter and an odd integer respectively. These geometries put longer antennas in a limited volume.

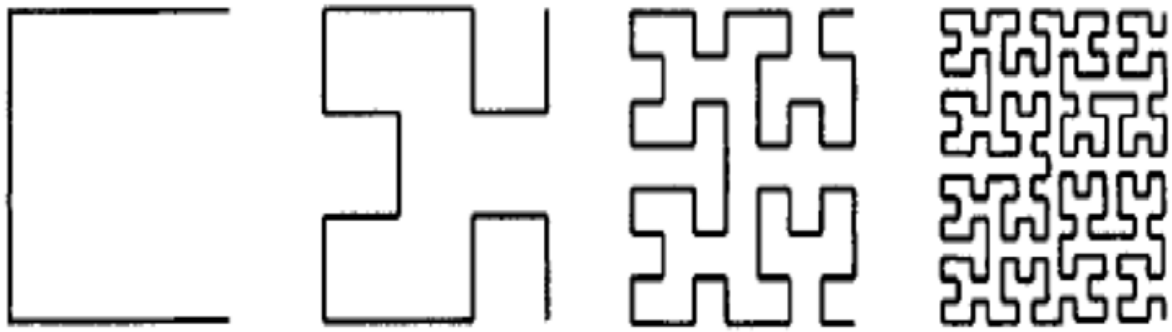

Figure 1.8 Four iterations of Hilbert Fractal Antenna [14].

1.6.5 Pythagorean Tree

Fractal antennas utilizing Pythagorean tree is novel design for multiband and wide band properties. This structure in made utilizing the Pythagoras theorem where three squares when consolidated in an appropriate way they enclose a right angle triangle as represented in Figure 1.8. This structure is easy to design, mode and fabricate. The utilization of appropriate feeding technique and slots helps is obtaining improved results [15]. This antenna has demonstrated exceptionally helpful for those applications which require high gain with large bandwidth and small size of antenna is another feature for its simple utilization. The design equations for designing pythagorean tree are mentioned in C.A Balanis and given here:

Resonant frequency can be given as:

$$f_r = \frac{c}{2L_{eff}\sqrt{\epsilon reff}}$$ Equation (1.5)

The effective dielectric constant is calculated by the formula which is as given below

$$\frac{W}{h} > 1$$

$$\epsilon_{reff} = \frac{\epsilon_r + 1}{2} + \frac{\epsilon_r - 1}{2}\left[1 + 12\frac{h}{w}\right]^{-1/2}$$ Equation (1.6)

A practical and very popular relation for extension of length is

$$\frac{\Delta L}{h} = 0.412\frac{(\epsilon reff + 0.3)\left(\frac{W}{h} + 0.264\right)}{(\epsilon reff - 0.258)\left(\frac{W}{h} + 0.8\right)}$$ Equation (1.7)

$$Leff = L + 2\Delta L$$

The values of length and width of the patch is given by

$$W = \frac{v}{2f_r}\sqrt{\frac{2}{\epsilon r + 1}}$$ Equation (1.8)

$$L = \frac{v}{2f_r\sqrt{\epsilon_{eff}}} - 2\Delta L$$ Equation (1.9)

L_{eff} = Effective length , V = speed of light which is 3X10 ^{8} m/sec , ϵ_r = relative permittivity

The length and width of ground is given

$$Lg = 6h + L$$ Equation (1.10)

$$Wg = 6h + W$$ Equation (1.11)

Where h presents thickness of substrate, L and W presents length & width of patch

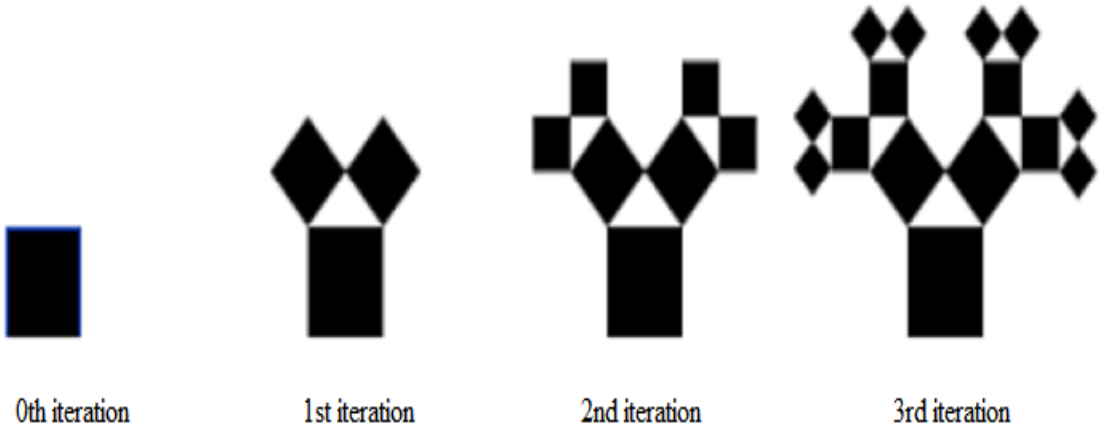

Figure 1.9 Four iterations of Pythagorean Fractal Patch Antenna [15].

1.7 MICROSTRIP PATCH ANTENNA PROPERTIES

There are several factors that determine antenna performance. Properties of those factors are discussed below:

1.7.1 Directivity

Directivity (D) of antenna determines a capacity of antenna to radiate energy. It is defined as ratio of maximum power radiated to power transmitted by reference antenna [16]. The

isotropic antenna is considered as reference antenna and radiates same energy in every direction with D as 100 % or 1. D is numerically characterized by the following equation:

$D = F_{max} / F_0$

Where F_{max} represents the maximum radiated energy and F_0 represents energy radiated by the isotropic antenna.

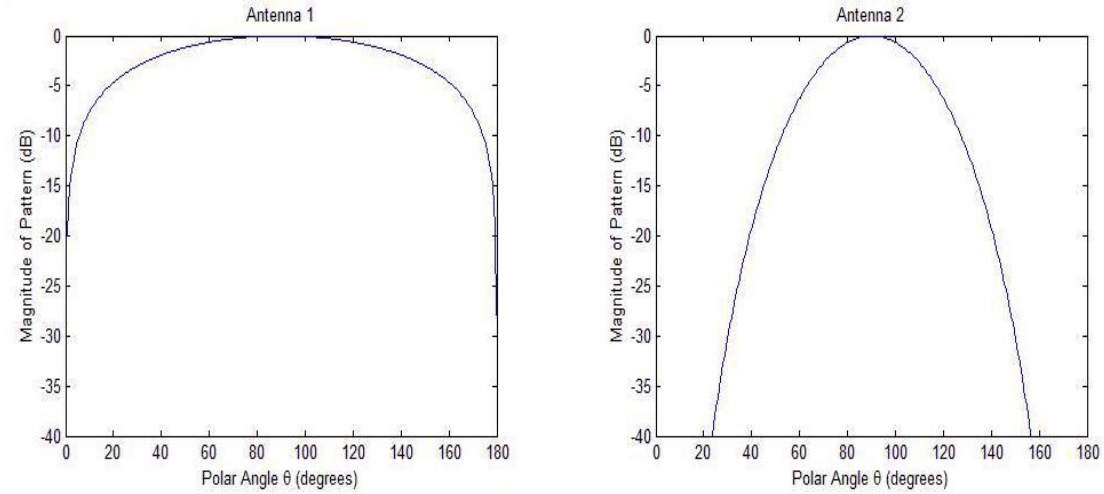

(a) (b)

Figure 1.10 Directivity of (a) Antenna 1 (b) Antenna 2 [16].

Figure 1.10 (a) & (b) show directivity plots of two antennas along the elevation plane. Antenna 2 has a better directivity.

1.7.2 Gain

The measure of radiation proficiency of antenna is considered as gain of antenna. The gain is equal to directivity for 100% efficient antenna. The overall efficiency of antenna is effected by many factors such as impedance bandwidth, network loss, material loss etc. with also degrades antenna performance [32].

1.7.3 Input Impedance

The input impedance is considered to determine maximum power transfer between transmission line and antenna. When input impedance of antenna and transmission line matches this transfer occurs. In case they do not match the antenna terminal will generate reflected wave and travel back towards the source [33-36]. The reduction in overall efficiency of system caused due to reflection needs to be avoided.

1.7.4 Polarization

The orientation and sense of radiated wave's electric field vector is depicted by antenna polarization [16]. The three basic polarizations are:

• Linear Polarization

• Elliptical Polarization

• Circular Polarization

Most of the antennas radiate with linear and circular. Linear polarized antennas radiate in same plane with wave propagation direction.

1.7.5 Bandwidth

The frequency range over which a certain set of specifications for antenna are met is termed as bandwidth. The antennas are considered as narrowband and wideband in terms of bandwidth [16]. It is considered broadband if $f_h/f_l \geq 2$.

Narrowband by percentage

$$BW = \frac{(f_h - f_l)}{f_0} \times 100\% \qquad \text{Equation (1.12)}$$

Broadband by ratio

$$BW = \frac{f_h}{f_l} \qquad \text{Equation (1.13)}$$

Where f_0 is the operating frequency, f_h is the higher cut-off frequency and f_l is the lower cut-off frequency

UWB was once known as "Pulse radio". The International Telecommunication Union Radio correspondence Sector (ITU-R) at present characterizes UWB [16] regarding transmission from antenna for which produced signal bandwidth capacity exceeds lesser of 20% of centre frequency or a bandwidth of 500 MHz.

1.8 FEEDING TECHNIQUES FOR MICROSTRIP PATCH ANTENNAS

MPAs are fed by variety of strategies that are extensively characterized into two fundamental classes, specifically, contacting and non-contacting. In contacting strategy, RF power is fed directly to radiating element utilizing a connecting component, for example, a microstrip line [16]. In non-contacting strategy, electromagnetic field coupling is done to transfer power between microstrip line and radiating element. The four most prevalent feeding strategies utilized are microstrip line, coaxial probe (both contacting techniques), aperture coupling and proximity coupling (both non-contacting techniques). These are represented in succeeding section.

1.8.1 Microstrip Line Feed

In this sort of feeding procedure, a leading strip is associated directly to the edge of the microstrip patch as appeared in Figure 1.11. This strip is smaller in width when contrasted with patch. The significant preference of this technique is that it can be etched on same substrate to form a planar structure.

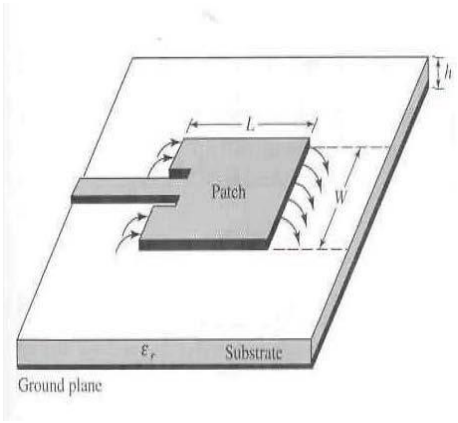

Figure 1.11 Microstrip Line Feed[16].

In many designs inset cut feed is favored over edge feed. The reason for inset cut is impedance matching of feedline to patch without requirement for any extra matching component. It is a simple feeding procedure for modeling and fabrication as well as for impedance matching.

1.8.2 Coaxial Feed

Another contacting scheme for feeding patch antenna is coaxial feeding technique. The design for this feeding technique is presented in the Figure 1.12. The coaxial connector in the inner conductor is extended through dielectric substrate and soldered to radiating element, whereas the ground plane is connected to the outer conductor.

To match the input impedance the feed can be placed at any desired location in the patch. The main advantage of this feeding technique is its ease of fabrication and low spurious radiation.

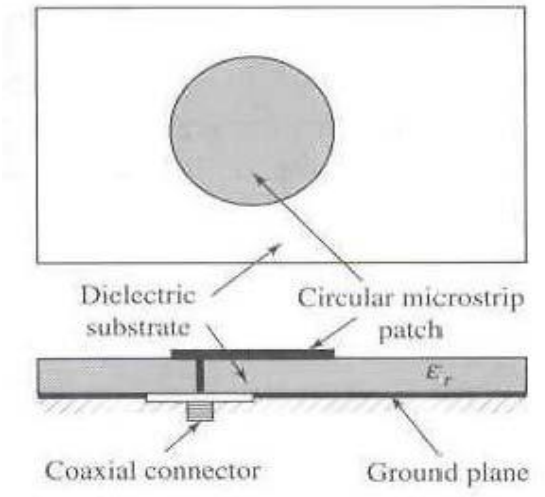

Figure 1.12 Coaxial Probe Feed [16].

The drawback of this technique is that its modeling is difficult and it provides narrow bandwidth, moreover hole drilled in the substrate and connector protrudes outside ground plane not making it completely planar. Additionally, for thicker substrates, the expanded probe length makes the input impedance more inductive, leads to matching issues. It is viewed as over that for a thick dielectric substrate, which gives expansive bandwidth; the

microstrip line feed and coaxial feed experience various disadvantages. The non-contacting feeding techniques which have been represented below take care of these issues.

1.8.3 Aperture Coupled Feed

In this kind of feeding method, the patch and MPAs feed line are isolated by the ground plane as appeared in Figure 1.13. Coupling between the patch and the feed line is made through a slot or an aperture in the ground plane.

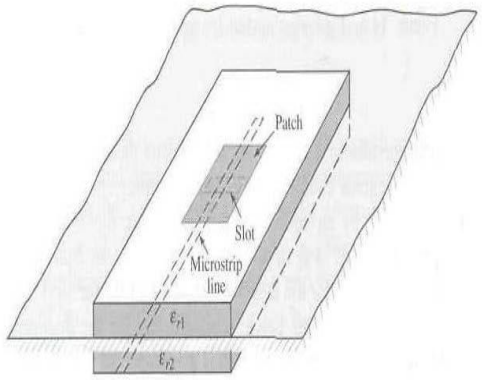

Figure 1.13 Aperture Coupled Feed for Patch Antenna [17].

The coupling aperture is generally centered under patch, prompting lower cross-polarization because of symmetry of the setup. The measure of coupling from feedline to patch is controlled by shape, size and area of aperture. Since ground plane isolates patch and feedline, spurious radiation is minimized [17]. For the most part, a high dielectric material is utilized for base substrate and a thick, low dielectric material is utilized for top substrate to enhance radiation from patch.

The significant drawback of this feed method is that it is hard to fabricate because of different layers, which additionally expands antennas thickness. This feeding technique additionally gives narrow bandwidth.

1.8.4 Proximity Coupled Feed

This kind feeding method is also known as electromagnetic coupling scheme, two dielectric substrates are utilized with feed line is between two substrates and patch is over upper substrate.

The fundamental preference of this feeding method is that it avoids spurious feed radiation and gives higher bandwidth in contrast with other feeding systems (as high as 13%), because of general increment in thickness of MPAs [16]. This plan additionally gives choices between two distinctive dielectric media, one for patch and one for feed line to advance individual performances.

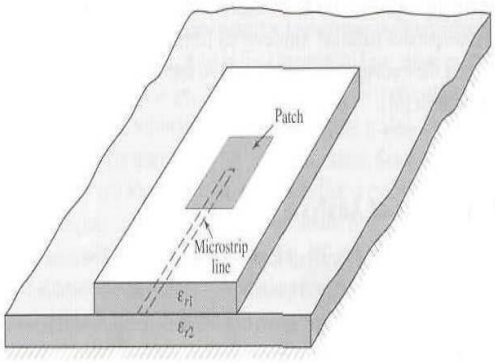

Figure 1.14 Proximity Coupled Feedline [16]

Impedance matching can be accomplished by controlling length of feedline and width-to-line proportion of radiating element. The real hindrance of this feeding technique is that it is hard to fabricate due to presence of two dielectric layers which require appropriate arrangement. Additionally, there is an expansion in general thickness of antenna.

Table 1.1 presents comparison of all above mentioned feeding techniques in terms of modeling, impedance bandwidth, impedance matching, spurious radiations, cost of fabrication and position of feedline [.

Parameters	**Microstrip Feedline**	**Co-axial Feedline**	**Aperture Coupled Feedline**	**Proximity Coupled Feedline**
Modeling	Easy	Easy	Difficult	Difficult
Bandwidth	Narrow	Narrow	Large	Large
Fabrication	Easy	Easy	Difficult	Difficult
Isolation between feed and patch	Low	Low	Good	Good
Matching	Easy	Easy	Difficult	Difficult
Spurious radiations	High	High	Low	Low

Table 1.1 Comparison of all Feeding Techniques.

As it can be observed from Table 1.1, an aperture coupled antenna provides reasonably higher bandwidth as compared to other feeds. Isolation between feed and patch is good as transmission of power to the radiating material is through aperture ground. It gives moderate spurious radiations with good impedance matching.

Micro-strip fractal antennas results in multiband frequencies and caters their applications in the field of any wireless communication such as WLAN, WiMAX, HIPERLAN, UWB and many more which are discussed in next subsection in detail with their respective frequency ranges.

1.9 APPLICATIONS OF MICROSTRIP PATCH FRACTAL ANTENNA

Advantages of fractal micro-strip aperture coupled antenna make them suitable for numerous applications. Telemetry and wireless communication antennas need to be thin and conformal and are often MSAs [37-46]. Fractal geometry results in close excitations of multiple frequencies which increases the overall bandwidth of the antenna. Thus using fractal antennas one can achieve ultra wideband without increasing the height of micro-strip antenna. Various applications covered in this thesis are mentioned in Table 1.2.

Band covered(in GHz)	Applications
2.2-4	S band. Various applications it covers are WLAN, WIMAX, wireless headphones, cordless phones, Bluetooth and many more.
3	Radio astronomy, UWB applications, radiolocation, civil and military [39, 40].
4 to 8	C band (For long distance radio communication, aeronautical military systems, passive sensors, telemetry)
5.15-5.8	Wireless local area networks, radio determination applications, feeder links for MSS, weather radar, Wi-Fi, HIPERLAN-2(Used for ATM access and security purpose)
6 to 8	H band (feeder links, radio determination, land military systems, weather satellites, satellite systems, land mobile)
8 to 12.4	X band [41-43] (used for satellite communication, radar, space communication ,global broadband system, unpaid radio system, molecular revolving spectroscopy)
12 to 18	K band (for radio determination, passive sensors, radio astronomy applications)

Table 1.2 Frequency bands covered by the Proposed Antenna.

1.10 RESEARCH GAPS

An extensive literature survey is carried out in chapter 2 that deals with the design and development of different types of fractal antennas for UWB applications.

A few research gaps that were identified are:

- The use of stacked MPAs and parasitic elements has proved to improve the bandwidth of antenna but it increases the overall size of antenna. Fractal geometries can be used for antenna miniaturization.

- Complex DGS has been used to achieve desired operational bandwidth. More work can be done in the field of DGS to achieve same results but with less complexity in ground plane.
- Slots in the ground plane effects the UWB behavior of fractal aperture coupled antennas. More work can be done on shaping of slots in ground plane.
- Improvement in gain is achieved at higher frequencies. So some technique can be applied to MPAs to increase the gain at lower frequencies.

1.11 THESIS OBJECTIVES

Based upon above discussed research gaps, following objectives had been designed to carry out thesis study:

- To study the use of fractal MSA for multiband and broadband operation.
- To design and simulate a plus shaped aperture coupled carpet fractal antenna for UWB applications.
- To design and simulate an aperture coupled Koch fractal antenna for UWB applications.
- To design and simulate an aperture coupled complementary bowtie antenna for UWB applications.
- To design a microstrip line fed cup shaped MSA with reduced DGS for UWB applications.
- Fabrication and testing of antennas.
- Application of these antennas to current wireless systems.

1.12 THESIS ORGANIZATION

The thesis is divided into following chapters:

- **Chapter 1:** Presents an overview of wireless communication, MPAs, fractal antennas.
- **Chapter 2:** Presents the literature survey.
- **Chapter 3**: Presents design, simulation and analysis of an aperture coupled plus shaped carpet fractal antenna, Koch aperture coupled fractal antenna, complementary bowtie aperture coupled fractal antenna and cup shaped microstrip line fed antenna.
- **Chapter 4:** Presents the fabrication and testing of plus shaped carpet fractal antenna and complementary bowtie fractal antenna using PCB technology and VNA respectively. Comparative study of simulated results and measured results is done.

- **Chapter 5:** Concludes the work done in this thesis and a brief discussion on the future scope of the present thesis work.

CHAPTER-2
LITERATURE SURVEY

Microstrip antenna gained its popularity because of its light weight, small size, coplanar structure etc. lot of research has been done by scientist in recent years. Comparison of various feeding techniques shows that aperture coupled feeding method is the best out of all the four. So this chapter presents a literature survey on the basics of MPAs, followed by use of aperture coupled feed, fractal MPAs and then the use of various fractal antennas for UWB applications.

2.1 MICROSTRIP PATCH ANTENNA

Siakavara K. *et al* in [3] presented brief study of MPA for various wireless applications. Various techniques are analyzed for designing MPA which make them suitable for modern communication applications. Each feeding technique and method of analysis was also studied briefly.

Balanis C.A. main objective in [7] was to introduce the fundamental principles of antenna theory and apply them to the analysis, design, measurements of antenna. The most basic antenna characteristics such as gain, directivity, radiation efficiency, impedance, surface current and polarization has been discussed in brief. Discussion on various techniques and systems used in near-to-far field measurements and transformation is carried out in this article.

Tripathi V.S. *et al* in [16] presented the comparison study of MPA over conventional microwave antennas. Study on MSAs, types of MSAs, feeding techniques used for it, method of analysis and applications of antenna with its advantages and disadvantages over conventional antenna were presented here.

Patil V.P. in [46] presented a rectangular MPA with two slots embedded diagonally on its side surface as the efficient method for the enhancement of bandwidth of the patch antenna to meet prerequisite for wireless applications. The proposed antenna is simulated and analyzed using GENESYS software. The antenna characteristics such as VSWR, input impedance and S_{11} parameters are analyzed. The simulated result for the proposed antenna gives impedance bandwidth of 311 MHz whereas fabricated antenna gives the bandwidth of 286 MHz.

2.2 APERTURE COUPLED MICROSTRIP PATCH ANTENNA

Pozar D.M. *et al* in [8] described the design and fabrication process of a circularly polarized aperture coupled antenna for GPS applications. Antenna operated at two resonant frequencies of 1227 MHz and 1575 MHz. Further the proposed antenna was tested and results where compared with simulated ones.

Singh M. *et al* in [17] presented the design and fabrication process of microstrip aperture coupled patch antenna using 0.762 mm and 0.508 mm thick substrates at 10 GHz frequency. The design is optimized by varying antenna parameters using a 3D electromagnetic simulator. Further simulated and measured results were studied. A gain of 6.21 dBi at 10GHz was achieved and it was suitable for X band communication systems.

Kaur A. in [42] presented the design and testing of a semi-spiral G-shaped compact structure using CST MWS'10 software for WLAN, WiMAX and U-NII band applications. To achieve multi-frequency and broadband behavior, resonant slots in patch with aperture coupled feeding technique was considered. Testing of antenna was done using VNA. A gain of 4.5 Db was achieved for all the three applications.

Patil V.P. in [46] included the design and simulation of stacked aperture coupled MPA operating at 5.8 GHz frequency with impedance bandwidth of 340 MHz for WLAN and WiMAX applications. The effect of varying antenna parameters such as length, width and dielectric constant of the substrate material, effect of using stacked antennas was studied. Various antenna parameters (return loss, gain, directivity, VSWR, bandwidth, input impedance) were observed.

2.3 FRACTAL MICROSTRIP PATCH ANTENNA

Gianvittorio J.P. *et al* in [6] gave the brief study on fractal antennas and its various geometries. Fractal antennas with self-similarity property had same possibility as that of conventional MPA for accomplishing multi band behavior by using multiple radiating elements or relatively loaded patch antennas. The self-similar nature provides similar surface current distributions for various resonating frequencies and space filling property of fractal antenna increased the electrical length of the radiating element.

Puente C. *et al* in [11] presented a model on sierpinski fractal antenna. The model was designed and simulated to operate at multiple frequency bands. The behavior of the proposed antenna was studied with respect to the parametric variations of simulated antenna. The prototype was tested and fabricated.

Vinoy K.J. *et al* in [14] derived an approximate formulation for the known resonant frequency of a Hilbert curve fractal antenna. Hilbert curve fractals because of their self-similar structures could be used as small resonant antennas which was useful in VHF/UHF communication applications. Formula derived in this article could be further inverted to obtain design equations for proposed antenna for a specified resonant frequency.

Aggarwal A. *et al* in [15] designed a Pythagoras tree fractal antenna with CPW feed technique. The proposed antenna was designed to resonate at two frequencies of 2.4 GHz for WLAN/WiMAX applications and 3.5 GHz for WiMAX/ ultra-wide band applications. Fabricated antenna shows a good match with simulated antenna.

Werner D.H. in [18] described fractal antenna engineering which focused in two areas. The first area dealt with the design and analysis of fractal antenna elements and the second one dealt with application of fractal concept to the design of antenna arrays. Fractals are composed of many self-similar copies of the base shape antenna. Unique properties of fractal have been exploited to define a new class of antenna elements for multiband and wideband operation and that were compact in size.

Hohlfeld R.G. *et al* in [19] described that the self-similarity property of fractal antenna and origin symmetry are key geometric constraints in determination of frequency independence property of antenna. Frequency independence is not dependent on self-complementary property of fractal antenna but helps in smoothing out the impedance variations.

Kaur N. *et al* in [21] presented the modified plus shape sierpinski carpet fractal antenna for S and C band applications. The simulation was carried out using HFSS software. Antenna was simulated up to 3 iteration level. VNA was used to monitor measured results of the fabricated antenna. Measured results show that the proposed antenna resonate at 2.23 GHz, 4.75 GHz, 5.23 GHz, 6.61 GHz, 6.79 GHz and 9.58 GHz resonant frequencies respectively. Return loss, VSWR and radiation pattern was evaluated to observe the performance of antenna. Maximum gain for all six resonant frequencies is 15.27 dB.

Jagdeesha S. *et al* in [23] proposed a self-similar fractal antenna with two element array. A plus shape antenna with 2 iteration level of scaling factor 1/3 is designed with substrate thickness of 1.6 mm. Multiband frequency response was achieved for the proposed antenna with size reduction of 72.83%. Return loss, VSWR and gain of simulated antenna was studied. Simulated and experimental results were studied further.

Baliarda C.P. *et al* in [25] described the unique geometric properties of fractal. The behavior of Koch curve monopole antenna was analyzed numerically and experimentally. As the level of iteration on proposed antenna increases, the Q factor of antenna approached the fundamental limit for small antennas.

Sundaram A. *et al* in [30] proposed a Koch folded-slot antenna iterated up to 2 iteration level. The simulation result for all three iterations was studied. It was observed that a better impedance bandwidth was achieved as the iteration level was increased. Return loss achieved for all three iterations was 40 dB, 34 dB and 42 dB with a bandwidth of 1.211 GHz, 0.4 GHz and 0.34 GHz respectively.

Puente C. *et al* in [32] described the multiband behavior of sierpinski fractal antenna. Patch consists of triangular shape slots in it. Numerical and experimental results show that self-similar property of fractal results in similar current distribution for various resonant frequencies resulting in electromagnetic behavior of antenna.

Kaur A. *et al* in [38] gave the complete review of recent developments in the field of fractal antenna engineering. A brief introduction about fractals with its designs and algorithms used for optimization and work done in this field of fractals was discussed.

Kaur A. *et al* in [39] proposed a aperture coupled stacked sierpinski gasket fractal antenna with DGS for UWB and WLAN applications. Antenna was designed and simulated using CST MWS'10 software. Dual wideband behavior with a bandwidth of 630 MHz and 400 MHz was observed. Gain of 5.85 dB and 9.5 dB for the two bands was achieved. Measured results were in good agreement with the simulated ones.

Anguera J. *et al* in [40] discussed the unique properties of fractal antenna for advance wireless communication system. Further performance in terms of antenna size, gain,

multiband behavior using fractal geometries was studied in detail. A sierpinski bowtie fractal antenna was presented in this article.

2.4 FRACTAL MICROSTRIP PATCH ANTENNA FOR UWB APPLICATIONS

Yadav S. *et al* in [13] presented a Koch curve fractal antenna for UWB applications. Different iterations for designing proposed antenna was discussed. A omni-directional radiation pattern with acceptable gain was achieved. It was fabricated on a FR4 substrate material having dimensions 33.5×28.5×1.6 mm^3. It covered C band applications (2.8-6.4 GHz) and WiMAX (3.4-3.69 GHz).

Jagadeesha S. *et al* in [22] outlined a multiband fractal antenna design. A plus shaped microstrip antenna was designed and simulated using IE3D software. Antenna radiated at multi resonant frequencies. Using fractal antennas, 82.6% of size reduction and bandwidth of 33.8 was achieved. A good match between the simulated results and experimental results was observed.

Cohen N. in [27] states that by applying fractal geometry to conventional antenna elements, it results in size miniaturization of antenna, improved bandwidth, better input impedance and multiband resonant frequencies without changing the physical length of the antenna. Merits and demerits and its application in the field of wireless communication system were discussed.

Choukiker Y.K. *et al* in [33] presented a microstrip line feed sierpinski square fractal antenna with band notch characteristics for ultra wideband applications. Proposed antenna covered the frequency range of 3.1-10.6 GHz with impedance bandwidth of 7.5 GHz and radiation pattern obtained is omni-directional. ∩-slot is inserted in feedline to obtain the desired results.

Bisht A. *et al* in [44] presented a novel cup shape slotted antenna for UWB applications. Proposed design contained a radiating patch with cup shape slot in it. An ultra wideband ranging from 2.45-10.9 GHz was achieved. Simulated results and measured results were further studied.

Azari A. in [45] designed an octagonal fractal antenna for achieving multiband and broadband and UWB applications. The simulation and optimization was carried out using

CST MWS. Proposed antenna covered a frequency range of 10-50 GHz with 40 GHz bandwidth resulting in a super wideband antenna. Gain and radiation pattern was also discussed.

Patil V.P. in [46] discussed the efficient methods used for the enhancement of patch antenna bandwidth. Two square slots across patch side surface were inserted for bandwidth improvement. The VSWR, gain, input impedance and return loss were also studied for analysis of antenna performance. Simulated results gave the impedance bandwidth of 311 MHz whereas the measured results give the impedance bandwidth of 286 MHz.

2.5 CONCLUSION

This chapter presented the literature survey carried out in the field of aperture coupled MSAs and Fractal MSAs. Based on the research gaps and survey identified, the objectives for research were defined to carry out research work mentioned in further chapters.

CHAPTER 3

DESIGN AND SIMULATION OF MICROSTRIP ANTENNAS FOR UWB APPLICATION

3.1 INTRODUCTION

This chapter presents the design and simulation results of four UWB antennas namely plus shaped carpet fractal antenna, Koch fractal antenna, bowtie fractal antenna and cup shaped micro-strip patch antennas is presented. The proposed plus shaped carpet fractal antenna covers C & X band suitable for various applications with multiple frequencies band at (4.83-5.06 GHz), (6.09-6.43 GHz) and (6.93-11.39 GHz). It caters its applications in the field of wireless communication, satellite communication, radar communication and ultra wideband applications. The Koch fractal antenna covers the impedance bandwidth of 3900 MHz covering the frequency range from 5.3-9.28 GHz for ultra wideband applications [42], feeder links, land mobile, satellite communication, feeder links for MSS and radio determination applications. The bowtie fractal aperture coupled antenna covers the impedance bandwidth of 1700 MHz covering the frequency range from 3.6-5.3 GHz for radio astronomy, UWB applications, passive sensors, telemetry, HIPERLAN-2, weather radar applications. The cup shaped micro-strip patch antenna covers the impedance bandwidth of 21 GHz covering the frequency range from 4.9 -25.9 GHz for X band, Ku band and K band applications. Design and simulation of these antennas is done using CST MWS V'14 and simulation results are presented.

3.2 DESIGN EQUATIONS

Transmission line model is used to describe the mathematics behind working of MSA. This has an advantage of being simple but lacks versatility in some cases. According to transmission line model, along the length and width, the dimensions of patch are finite and therefore at the edges of the patch the fields undergo fringing [3]. The EM waves move in air & substrate too. Due to this the dielectric constant is not considered but effective dielectric constant of material is considered for fringing effects and wave propagation. The effective dielectric constant is calculated by the formula which is as given below in Equation (3.1).

$$\frac{W}{h}>1$$

$$\epsilon_{reff} = \frac{\epsilon r+1}{2} + \frac{\epsilon r-1}{2}\left[1+12\frac{h}{w}\right]^{-1/2} \qquad \text{Equation (3.1)}$$

Due to fringing effects, the patch of the antenna looks electrically greater than the physical dimensions of the patch. A practical and very popular relation for extension of length is

$$\frac{\Delta L}{h} = 0.412\frac{(\epsilon_{reff}+0.3)\left(\frac{W}{h}+0.264\right)}{(\epsilon_{reff}-0.258)\left(\frac{W}{h}+0.8\right)}$$ Equation (3.2)

$$Leff = L + 2\Delta L$$

Where

h= thickness of the substrate, W= Width of the patch, L = Length of the patch, Leff= Effective length, v= speed of light which is 3X10 ^{8} m/sec, $\in$ r = relative permittivity, $\in$ eff = effective permittivity

The values of length and width of the patch is given by

$$W = \frac{v}{2fr}\sqrt{\frac{2}{\in r + 1}}$$ Equation (3.3)

$$L = \frac{v}{2fr\sqrt{\in eff}} - 2\Delta L$$ Equation (3.4)

This model is related to only those ground planes which are infinite. For practical considerations, it is necessary that there should be a finite ground plane. It is found that for both infinite and finite ground planes same results can be obtained if the dimensions of the ground is greater than the patch dimensions by nearly six times the thickness of the substrate all around periphery[8]same. Therefore, the length and width of ground is given

$$Lg = 6h+L$$ Equation (3.5)

$$Wg = 6h+W$$ Equation (3.6)

Lg= Length of ground

Wg= Width of ground

Design Equation for calculating Equilateral Triangular for the proposed antenna

The side of equilateral triangular notch for dominant TE10 is evaluated using following equation:

$$A = \frac{2c}{3f_r\sqrt{\varepsilon_r}}$$ Equation (3.7)

where A is side of triangle, $f_r$is resonant frequency ,ε_r is dielectric constant of substrate and c is speed of light.

3.3 DESIGN AND SIMULATION OF A PLUS SHAPED FRACTAL ANTENNA FOR UWB APPLICATIONS

This subsection presents the designing and simulation results of a defected ground structure plus shaped fractal antenna with aperture feed for UWB applications [21]. Designing is done in CST MWS V'14. The substrate chosen is FR-4 with dielectric constant equal to 4.4 and thickness equal to 1.6mm. The thickness of the conducting material is taken equal to

0.035mm. The simulation results are analyzed in terms of return loss, bandwidth, smith chart, gain and current distribution.

3.3.1 Antenna Design and Specifications

The main aim of the antenna design presented here is to design a MSA for UWB applications which support a good data rate for current wireless scenario. The designing starts with choosing of a basic '+' shape which is based on the design equations discussed in section 3.2. The base antenna is indicated in the Figure 3.1. The zeroth iteration patch is premeditated by Boolean addition of two slots in plus shape. Further a horizontal slot is inserted on both sides of the base shape antenna with respect to the center of the base plus shaped patch. The optimized distance between the two horizontal slots is calculated to be q=3mm. The size of the substrate used is 27.5mm×42.5mm. Figure 3.1 represents the three levels of iterations i.e 0th iteration, 1st iteration and 2nd iteration. Figure 3.2 represents the middle view of the ground plane with an I shaped slot and back view of feedline. Dimensions of each iteration are decreased to 1/3rd of its base frame. As the iteration level increases, the resonant frequency becomes lower which represents a conventional plus shaped patch. The optimized dimensions of various antenna design parameters are specified in Table 3.1.

Figure 3.2 shows the view of ground plane for the aperture coupled antenna. For optimization purpose, slot in the ground is modified to an I shape to achieve UWB results.

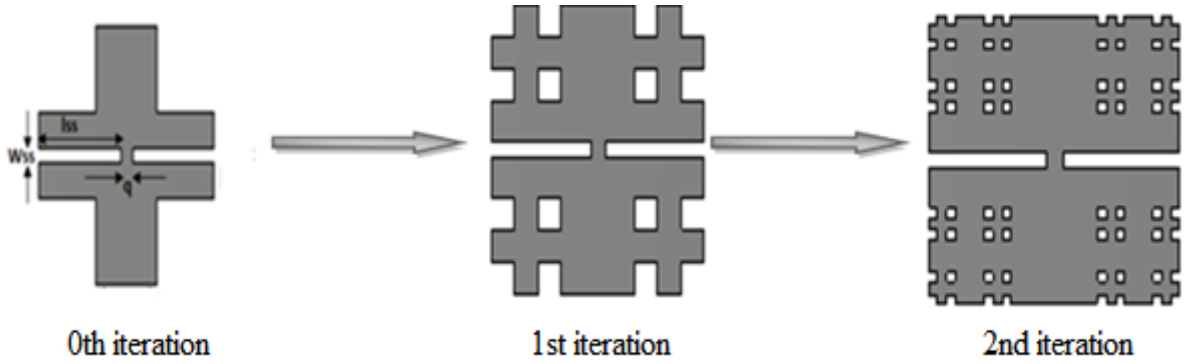

Figure 3.1 Design Steps of Plus Shaped Fractal Antenna.

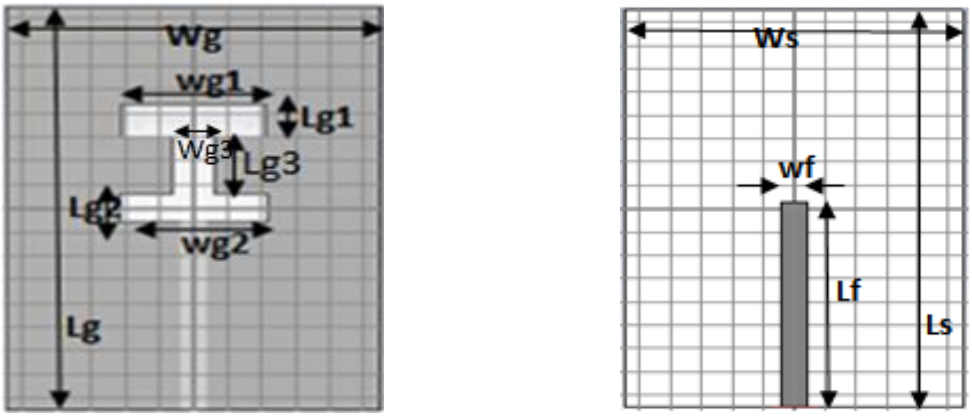

Figure 3.2 Middle view of Ground Plane and Back View Of Aperture Coupled Feed-Line.

Parameters	Dimensions
Wg	55mm
Lg	84mm
Wg1	21.5mm
Wg2	22mm
Lg1	7mm
Lg2	6mm
Lg3	9mm
Ws	55mm
Ls	84mm
Wf	4mm
Lf	41mm
Wss	2mm
Lss	21.675

Table 3.1 Design parameters of the Optimized Antenna.

3.3.2 Simulation Results and Discussion

The antenna design discussed above is simulated using CST microwave studio version 2014 and Simulation results in terms of impedance bandwidth, smith chart, current distribution and gain are presented in this section.

3.3.2.1 Impedance Bandwidth

The antenna is a carpet fractal that is optimized up to three iterations (0 to 2), the impedance bandwidth plot obtained is shown in Figure 3.3. Figure 3.3 shows a combined plot of S_{11}(dB) of the antenna for all three iterations of carpet fractal. Since the optimized results in terms of impedance bandwidth are obtained at the 2nd iteration with a scaling factor of 1/3, this stage is considered as the optimized one.

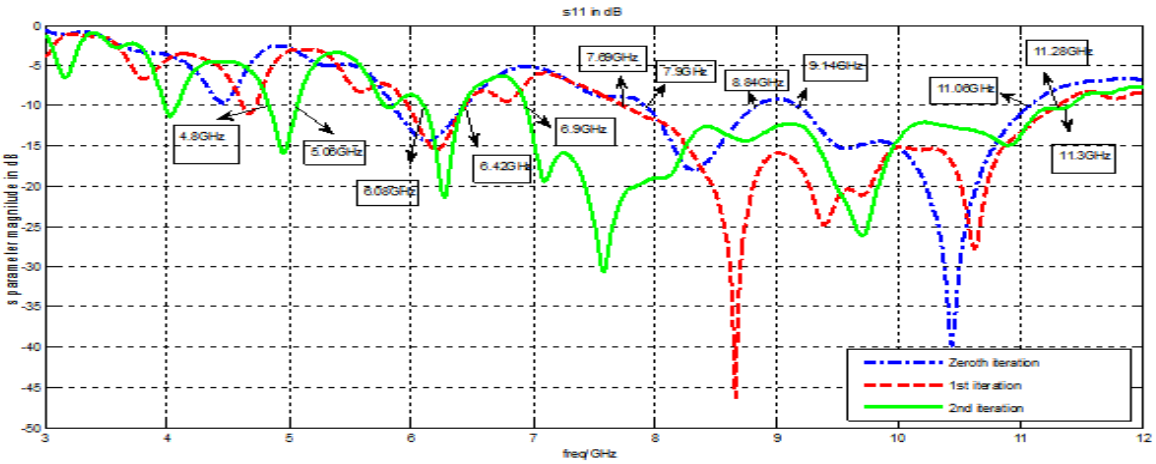

Figure 3.3 Simulated return loss graph for three level iterations.

The dark line in the Figure shows the S_{11}(dB) plotted against frequency for 2nd iteration. The optimized antenna covers the frequency band ranging from 3.9-4.08 GHz, 4.8-5.06 GHz, 6.1-6.4 GHz, 6.93-11.39 GHz with adequate bandwidth of 180 MHz, 260 MHz, 300 MHz and 4460 MHz respectively. Use of carpet fractal geometry with multiple plus shaped metal patch of scaled order (1/3) allows multiple current loops to be generated on the patch. This allows a better fringing effect and hence a higher bandwidth is exhibited by the antenna at 2nd iteration level.

3.3.2.2 *Smith chart*

Figure 3.4 show a smith chart plot of the simulated carpet fractal to the second order of iteration. Markers show the resonant frequencies at 4.01GHz, 6.25GHz, 7.5 GHz and 9.6 GHz respectively of the optimized antenna. The antenna is matched to a standard impedance of 50ohms for providing a best radiation efficiency.

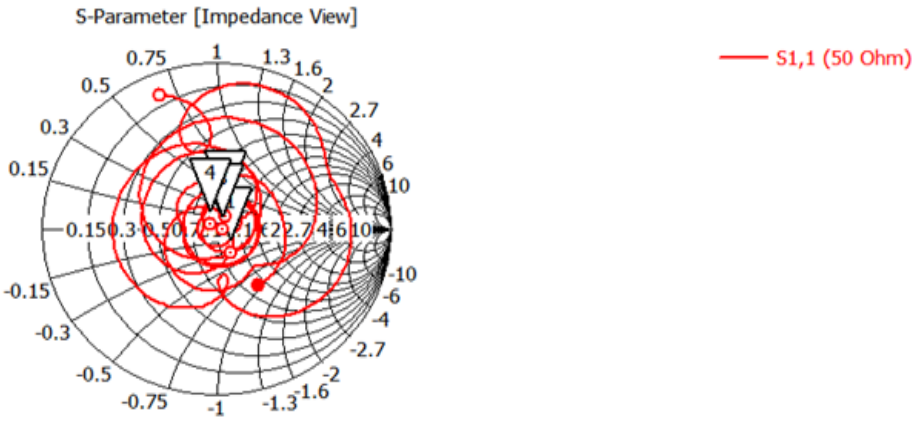

Figure 3.4 Smith chart for the Proposed Antenna.

3.3.2.3 Gain

The Figure 3.5(a) shows the broadband gain of antenna for entire set of frequencies of its operation. The peak gain is 3.99 dB at 7.9 GHz frequency and the average gain exhibited by this antenna is 1.05dB for the entire UWB of operation. A peak gain of 4 dB allows this antenna to be applicable for short range indoor wireless communication.

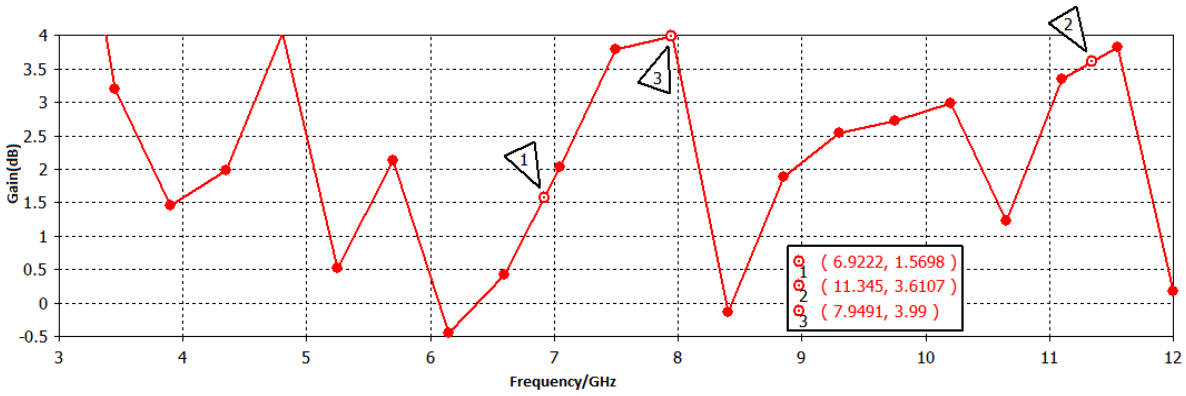

(a)

Figures 3.5(b) and 3.5(c) show the polar plots of the elevation and azimuthal plane view of the antennas radiation pattern at the frequency of 8GHz that shows a peak gain value of 4dB approx.

The antenna has a major lobe directed along θ = -31 degree with major lobe half power beamwidth of 125.1 degree. The elevation pattern shows a directional radiation pattern along the elevation plane. The antenna is directional along the azimuthal plane also that can be verified from Figure 3.5(c).

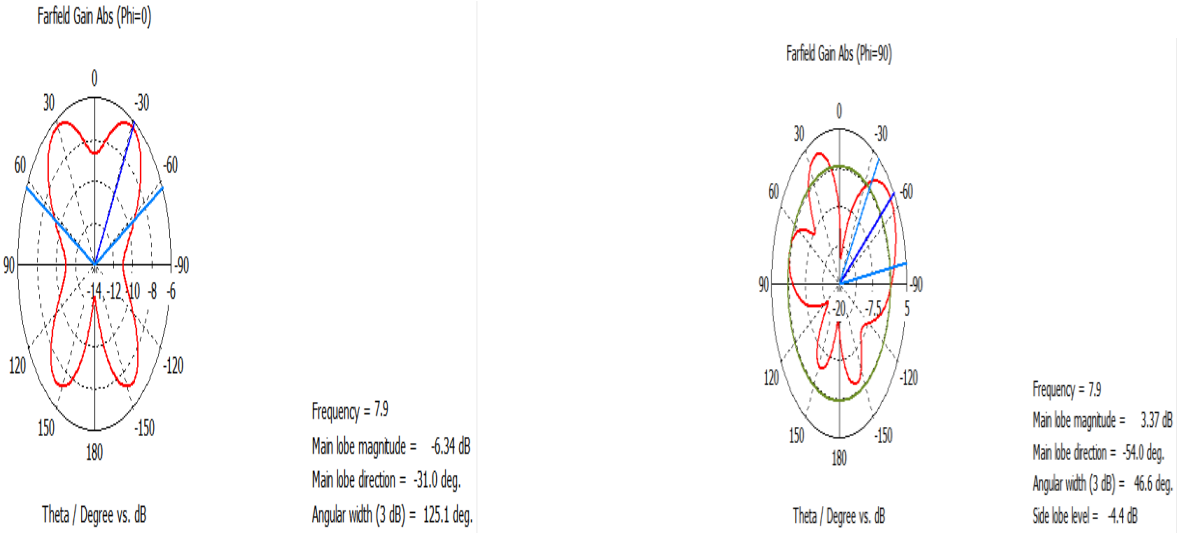

(b) (c)

Figure 3.5 Proposed Antenna for (a) Linear Gain Plot at 7.9 GHz for (a) polar plot for Elevation Plane (b) Polar Plot for Azimuthal Plane.

3.3.2.4 *Surface Current Distribution*

Figure 3.6(a-f) show current distribution on various layers of antenna for resonant frequencies of 7.5 GHz and 9.6 GHz when antenna is energized using an aperture coupled feeding in the software. A comparative study of surface current on various layers of antenna leads to the conclusion that top patch is responsible for exciting 7.5 GHz frequency. This can be verified from Figure 3.6(a) & 3.6(b) where current distribution on patch and ground is compared at 7.5 GHz. It can be noticed that maximum current flows at edges of the patch, which results in enchantment of the operational bandwidth. Similarly Figure 3.6(c) & 3.6(d) show the comparative study of the surface current on various layers of antenna at 9.6 GHz frequency. Thus it can be concluded that ground is responsible for exciting 9.6 GHz frequency. The maximum current flows at the boundary of I-Shaped DGS which results in the enhancement of operational bandwidth. Figure 3.6(e) shows comparative study of the surface current of aperture feed-line at 7.5 GHz and 9.6 GHz. It can be seen that feedline is responsible for exciting lower as well as higher frequency band resonating at 7.5 GHz and 9.6 GHz respectively and hence its optimization is helpful in getting the entire UWB.

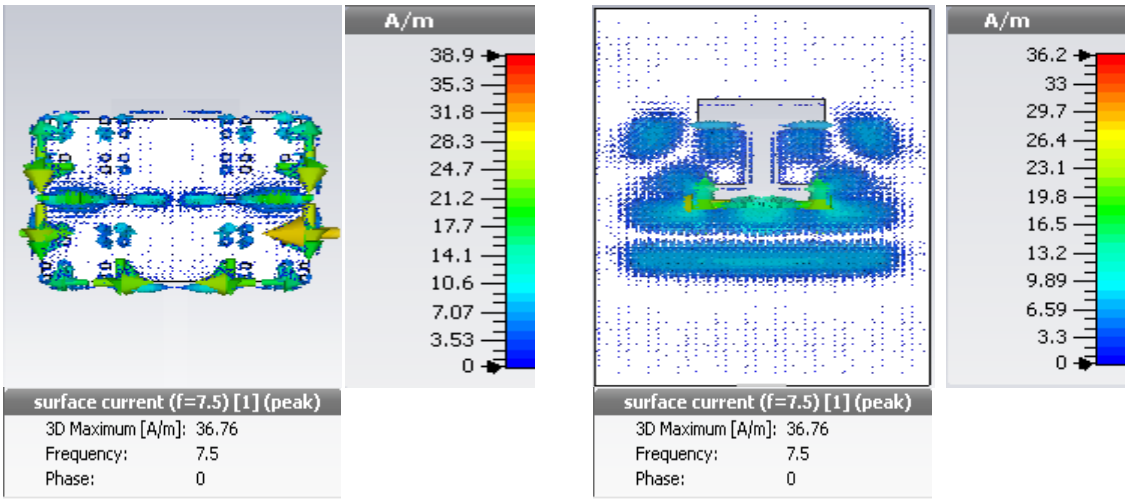

(a) (b)

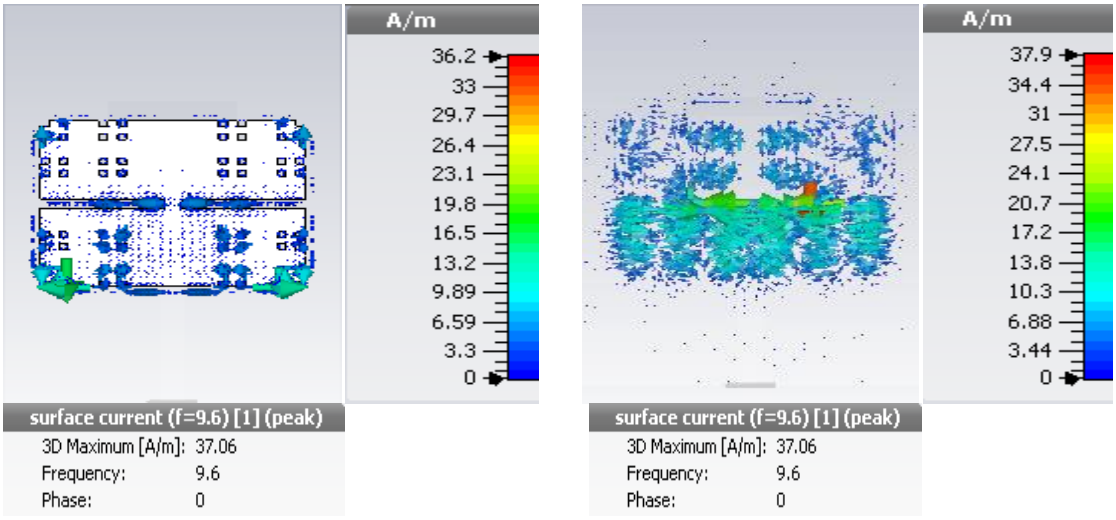

(c) (d)

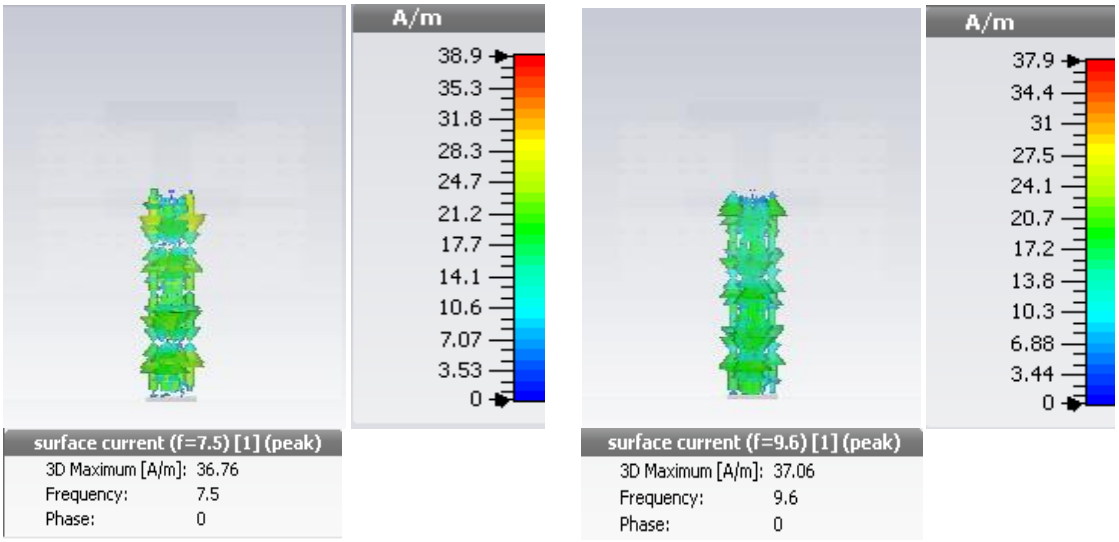

(e) (f)

Figure 3.6 Surface current distribution of the proposed antenna at resonating frequencies (a-b) 7.5 GHz (c-d) 9.6 GHz (e-f) 7.5 GHz, 9.6 GHz.

It is verified from surface current distribution plots that the current distributions on the plus shaped patch, I-shaped DGS and aperture feed-line at different resonating frequencies as

shown in Figure 3.6(a-e) is responsible for a multiband ranging from 4.8-5.06 GHz, 6.1-6.4 GHz and a ultra wideband ranging from 6.93-11.39 GHz with centre frequency at 9.6 GHz. I-shaped slot in the ground plane further enhances the bandwidth for the desired range. Thus it is concluded that as level of iterations increases bandwidth also increases.

3.3.3 Parametric Variations of the Proposed Plus Shaped Fractal Antenna for optimization

In this section, parametric variations of proposed antenna are carried out in order to achieve desired results for various wireless applications that cover the UWB.

3.3.3.1 *Variation of Proposed Antenna with And without I- shaped DGS*

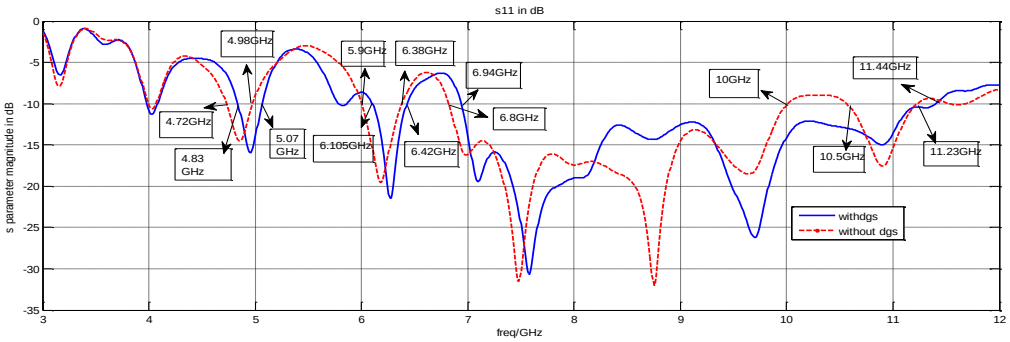

Figure 3.7 Comparison of S_{11}(dB) plot of antenna with and without I-shaped DGS.

The comparison of S_{11} dB plot of the antenna with and without DGS is shown in Figure 3.7. The dark line shows the S_{11}(dB) plot of the proposed antenna with I-shaped DGS whereas the dotted line shows the S_{11} plot without I-shaped DGS. It can be noticed that without I-shaped DGS, the antenna shows frequency bands ranging from 4.72-4.9 GHz, 5.9-6.3 GHz, 6.8-10 GHz and 10.5-11.23 GHz with impedance bandwidths of 180 MHz, 400 MHz, 3200 MHz and 730 MHz respectively. Whereas with that with I-shaped DGS slightly shifted and a wider band ranging from 6.93-11.39 GHz and a multiband ranging from 4.8-5.06 GHz, 6.1-6.4 GHz is covered with the bandwidth of 4460 MHz, 260 MHz and 300 MHz respectively. Thus I shaped DGS is responsible for achieving the better impedance bandwidth for the proposed antenna.

3.3.3.2 Varying Length of the Feed-Line

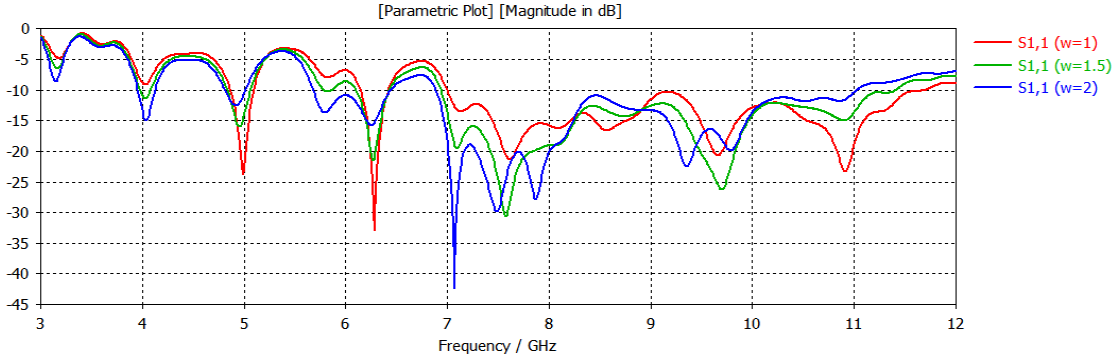

Figure 3.8 Comparison of S_{11} (dB) plot of the antenna by varying length of the feed-line

As illustrated in Figure 3.8, the variation in the length of the feed-line along y-axis results in the improved impedance bandwidth of the proposed antenna. The best optimized value is obtained at w=1.5 and it is kept fixed for the final designing of the proposed antenna. Thus by varying the length of the feed-line, improved antenna bandwidth is achieved.

3.3.3.3 Varying Wg2 in Ground Plane

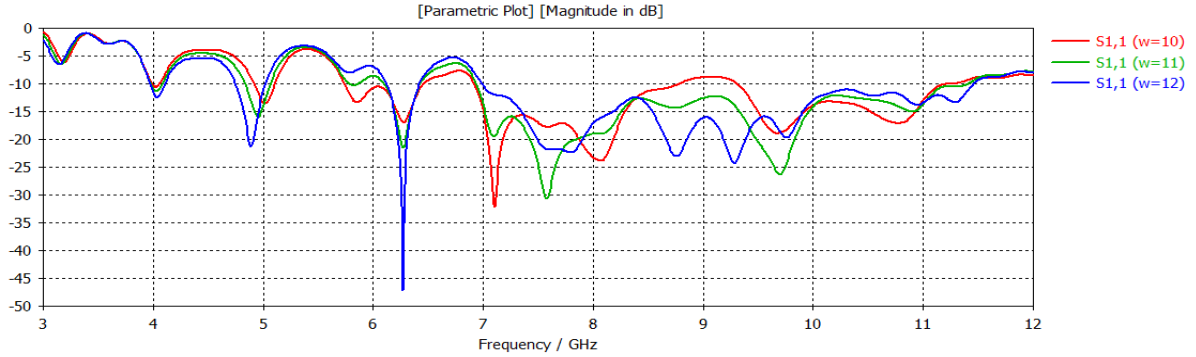

Figure 3.9 Comparison of S_{11}(dB) plot of the antenna by varying the width of slot1 in ground plane.

The Wg2 in ground plane is varied for three sample values as shown in Figure 3.9 to achieve the desired optimization antenna. It can be noticed that at w=10, the band is right shifted with poor impedance matching. At w=11 a wideband with better return loss value is obtained and at w=12 the band is left shifted with poor return loss. Thus the best optimized value obtained from these samples is at w=11mm.

3.3.4 Wireless Applications Covered by the Proposed Antenna

A plus shaped carpet fractal with I-shaped DGS covers C & X bands for various applications such as satellite communication, military systems and radar communication. C-band covers the frequency range of 4-8 GHz. In the proposed antenna frequency range covered is 4.8-5.06 GHz with its resonating frequency at 4.01 GHz for the application in the field of aeronautical military system. Frequency range covered from 6.1-6.4 GHz at resonating frequency at 6.25 GHz caters its application in passive sensor (satellite) field and frequency ranging between 6.93-11.39 GHz with its resonating at7.5 GHz and 9.6 GHz is applicable for UWB applications, radio determination application, amateur radio, terrestrial application and motion detectors used for traffic light detection.

3.4 DESIGN AND SIMULATION OF A KOCH FRACTAL APERTURE COUPLED MICROSTRIP ANTENNA FOR UWB APPLICATIONS

In this section, a Koch fractal aperture coupled antenna is designed and simulated using CST MWS V'14. The simulation results are analyzed in terms of return loss, bandwidth, smith chart, gain and current distribution.

3.4.1 Antenna Design and Specifications

The geometry of the proposed Aperture coupled-fed Koch fractal based slot antenna is illustrated in Figure 3.10. The antenna is designed on a low-loss FR4 substrate of thickness h=1.57mm and permittivity Ɛr=4.4. A Koch fractal slot is printed on one side of the substrate and is fed by aperture coupled feed along with a stub. The design procedure starts with an equilateral triangle of side 28mm and then another equilateral triangle of same length is attached to form a star shape and presents 0^{th} iteration as shown in Figure 3.10(a). Then this star shape patch is rotated at an angle of 45 degree for 2^{nd} iteration. A slot of side 14mm is cut at the centre for the final iteration. The basic geometry of the slot is an equilateral triangle of side 'a' which is calculated using equation discussed in section 3.2, on which repeated iterations lead to the Koch snowflake geometry as shown Figure 3.10(a). Figure 3.10(b) shows the ground layer. The size of aperture is modified to achieve desired results. a defect of 'T' shape is cut from the ground to make it a DGS. Figure 3.10(c) shows bottom view of feedline.

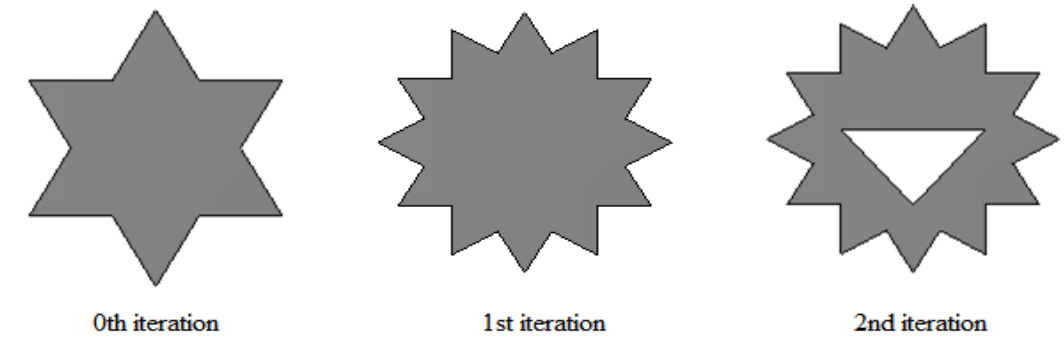

(a)

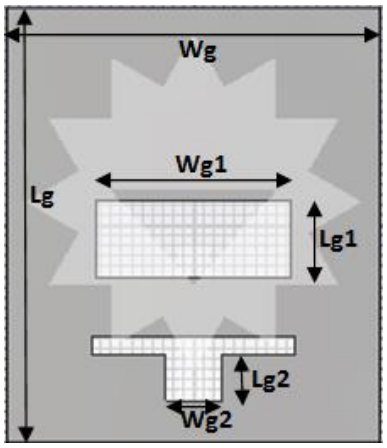

(b)

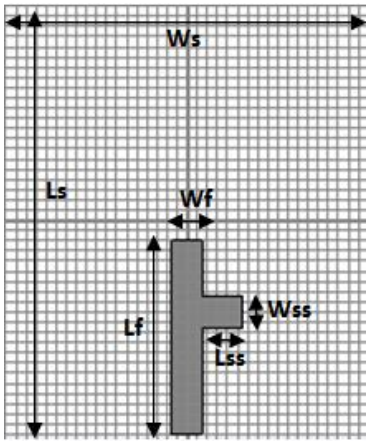

(c)

Figure 3.10 Proposed antenna design (a) Various level of iterations (b) middle view of ground plane (c) bottom view of aperture coupled feedline.

The various antenna parameters with their parametric values are discussed below:

Parameters	Dimensions
Wg	36mm
Lg	42mm
Wg1	19mm
Wg2	5.4mm
Lg1	7.4mm
Lg2	5mm
Ws	36mm
Ls	42mm
Wf	3mm
Lf	19mm
Wss	3mm
Lss	2mm

Table 3.2 Design Parameters of the Optimized Antenna.

3.4.2 Simulation Results and Discussion

All the simulation results related to antenna designs were carried out using CST MWS version 2014. The patch, ground plane, feed-line, aperture and tuning stub were optimized for the desired results. The results are presented in this section.

3.4.2.1 Impedance bandwidth

The antenna is a Koch fractal that is optimized up to three iterations (0 to 2), the impedance bandwidth plot obtained is shown in Figure 3.11. Figure 3.11 shows a combined plot of S_{11}(dB) of the antenna for all three iterations of Koch fractal. Since the optimized results in terms of impedance bandwidth are obtained at the 2nd iteration, this stage is considered as the optimized one and band is resonating at lower frequencies as compared to other 2 iterations.

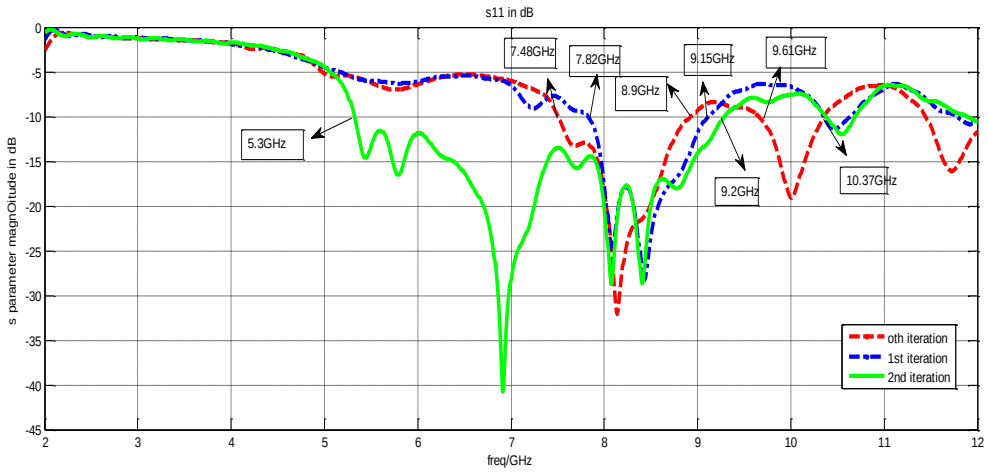

Figure 3.11 Simulated S_{11}(dB) Parameter.

The dark line in Figure 3.11 shows the S_{11} (dB) plotted against frequency for 2nd iteration. The optimized antenna covers the frequency band ranging from 5.3-9.2 GHz with adequate bandwidth of 3900 MHz resonating at 6.9 GHz, 8.0 GHz and 8.4 GHz respectively. Use of a Koch fractal geometry with triangular slot in it allows multiple current loops to be generated on the edges of patch and triangular slot. This allows a better fringing effect and hence a higher bandwidth is exhibited by the antenna at 2nd iteration level. The operating frequency covers the bandwidth of 53.7% which exceeds the required UWB range.

3.4.2.2 Smith Chart

Figure 3.12 shows the smith chart plot of the simulated carpet fractal antenna for the second order of iteration. Markers show the resonant frequencies at 6.9 GHz, 8.04 GHz and 8.4 GHz respectively of the optimized antenna. The antenna is matched to a standard impedance of 50ohms for the impedance bandwidth of 3900 MHz with a frequency range from 5.3-9.2 GHz.

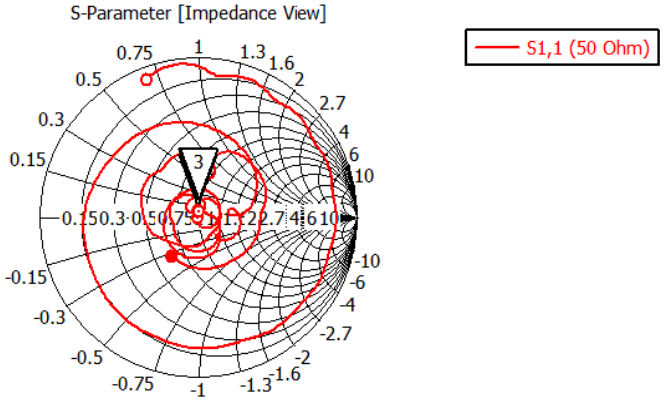

Figure 3.12 Smith chart of the Proposed Antenna.

3.4.2.3 Gain

The Figure 3.13 shows the broadband gain of antenna for entire set of frequencies of its operation. The peak gain is 4.5 dB at 6.49 GHz frequency and the average gain exhibited by this antenna is 3.9 dB for the entire UWB of operation. A gain of 4.5 dB allows this antenna to be applicable for short range indoor wireless communication.

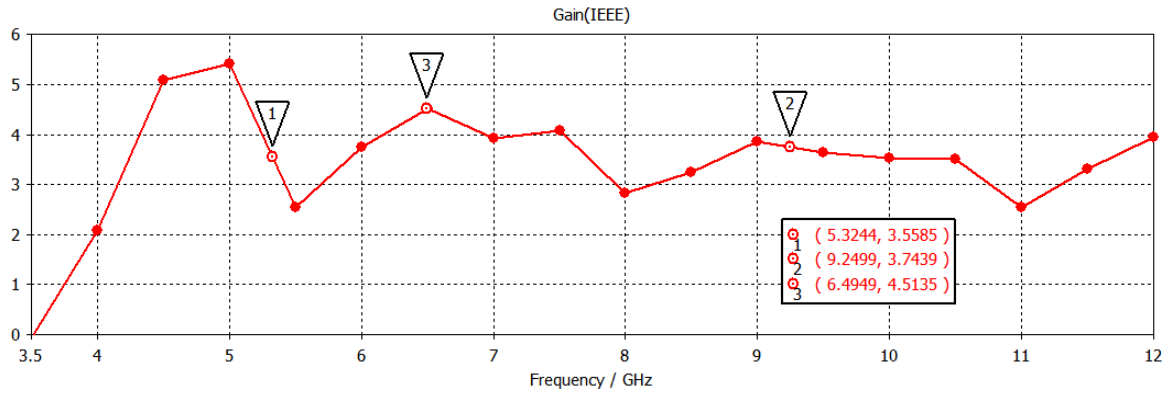

Figure 3.13 Simulated Peak Gain of Proposed Antenna.

Figure 3.14 (a) shows the 3D plot at the frequency of 6.49GHz that shows a peak gain value of 4.5 dB approx. Figure 3.14(b-c) shows the polar plot of proposed antenna for elevation and azimuthal plane at 6.49 GHz frequency. Figure 3.14(b) shows that the antenna has a major lobe directed along θ = -3 degree with major lobe half power beamwidth of 54.8 degrees. The elevation pattern shows a directional radiation pattern along the elevation plane. The antenna is directional along the azimuthal plane also that can be verified from Figure 3.14(c).

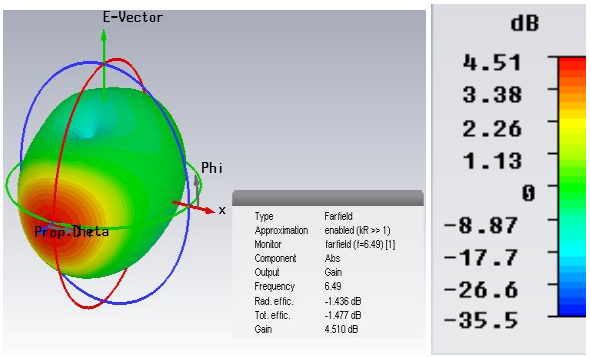

(a)

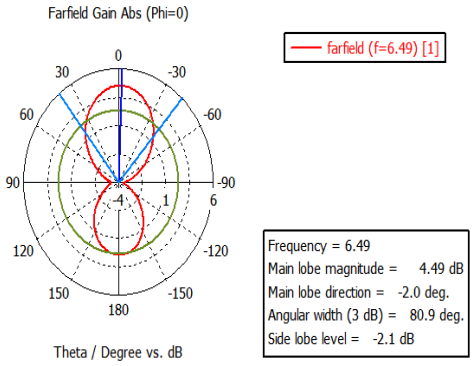

(b)

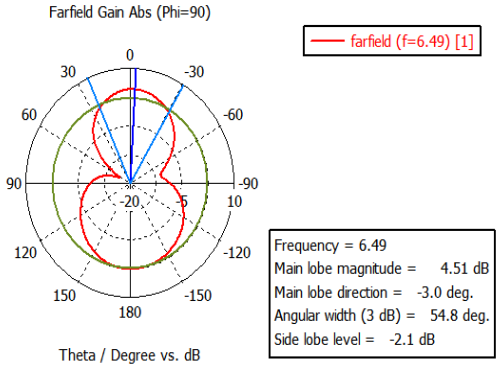

(c)

Figure 3.14 Proposed antennas for (a) 3D peak gain at 6.49 GHz frequency (b) Polar gain plot for Elevation plane at 6.49 GHz(c) Polar gain plot for Azimuthal plane at 6.49 GHz.

3.4.2.4 Surface Current Distribution

Figures 3.15(a-i) show surface current distribution on the various layers of antenna for resonant frequencies of 6.49 GHz, 8.04 GHz and 8.4 GHz when antenna is excited using an aperture coupled feeding in the software. It is demonstrated from Figure 3.15(a) that maximum magnitude of the current flows at the boundaries of the triangular slot at 6.49 GHz frequency. Figure 3.15(b), the current is flowing through the entire ground plane but the maximum current distribution is at the boundary of the T- shaped slot in the ground plane. Similarly in Figure 3.15(c), it can be seen that the maximum current distribution is seen on the stub of the feed-line at 6.49 GHz. In Figure 3.15(d), the current is evenly distributed through the entire edges of the radiating patch but the maximum magnitude of the current is

seen at the upper and lower edges of the patch at resonating frequency 8.04 GHz. Figure 3.15(e), it is examined that the maximum magnitude of the current is distributed on the upper boundary of the rectangular slot and on the edges of the T-shaped slot in the ground plane respectively at 8.04 GHz resonating frequency. Figure 3.15(f) reveals that the current is evenly distributed throughout the feed-line at 8.04 GHz resonating frequency. Figure 3.15(g) depicts that the maximum current is flowing through the entire edges of the Koch shaped fractal patch at 8.4 GHz resonating frequency. Figure 3.15(h), it is examined that the maximum current distribution is seen at the lower boundary of the T-shaped slot in the ground plane at a resonant frequency of 8.4 GHz. Similarly from Figure 3.15(i), it can be concluded that the current is evenly distributed through the entire feed-line for 8.4 GHz resonating frequency.

Thus the Figures 3.15(a-i) helps in explaining that stub part of feedline is responsible for resonant frequency of 6.49 GHz. The edges of the patch are responsible for resonant frequency of 8.04 GHz and the 'T' shaped slot in ground plane excites the 8.4 GHz frequency. Thus these nearby frequencies merge to form the required UWB of operation.

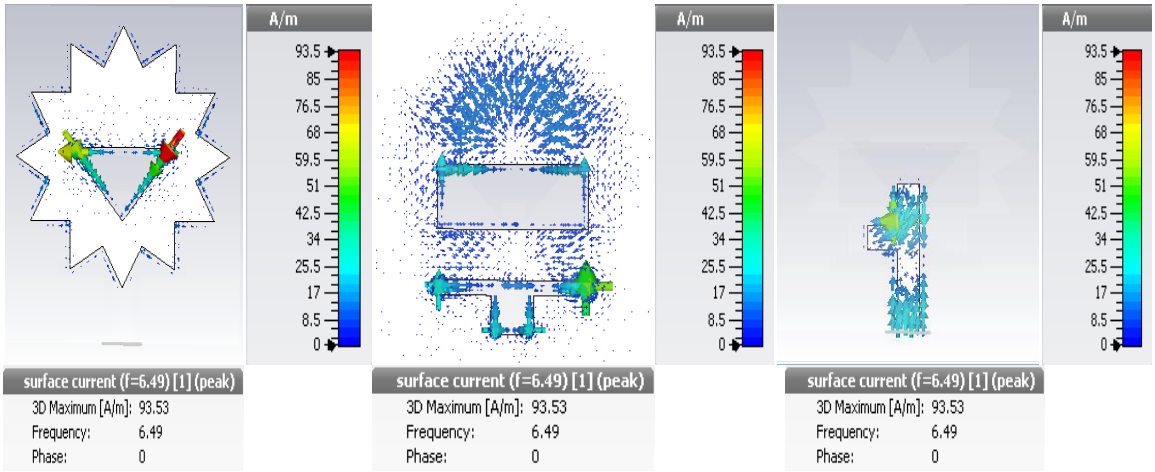

(a) (b) (c)

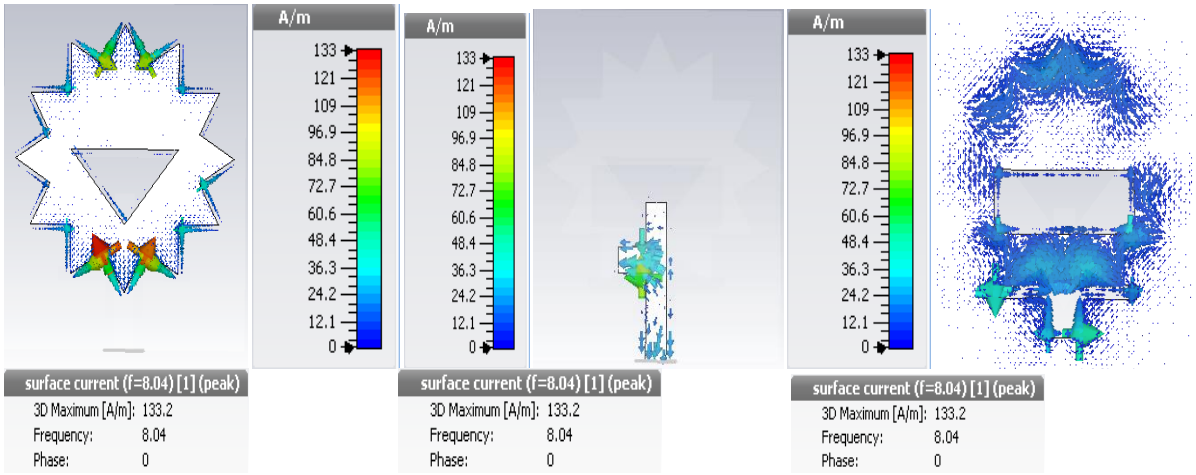

(d) (e) (f)

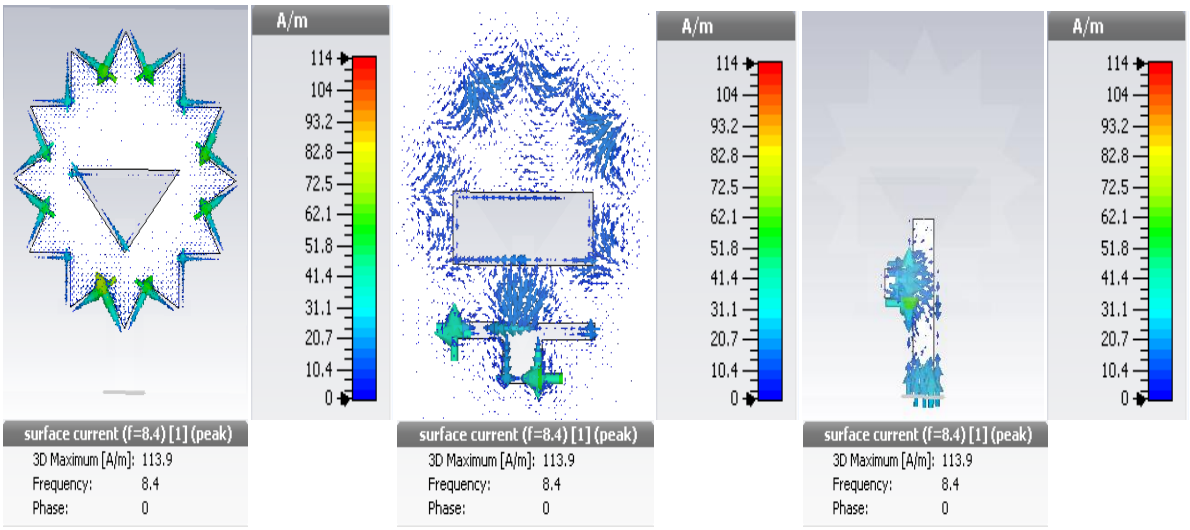

(g) (h) (i)

Figure 3.15 Surface Current Distribution of the Proposed Antenna at Resonating Frequencies (a-c) 6.49 GHz (d-f) 8.04 GHz (g-h) 8.4 GHz.

3.4.3 Parametric Variations of the Proposed Antenna

In this section, parametric variations of the proposed antenna such as length and width of ground plane, slots in ground plane, varying length and width of feedline and stub in the feedline, varying slots in patch etc are carried out in order to achieve the desired results for various wireless applications that cover the UWB.

3.4.3.1 Varying Wg1 in the Ground Plane

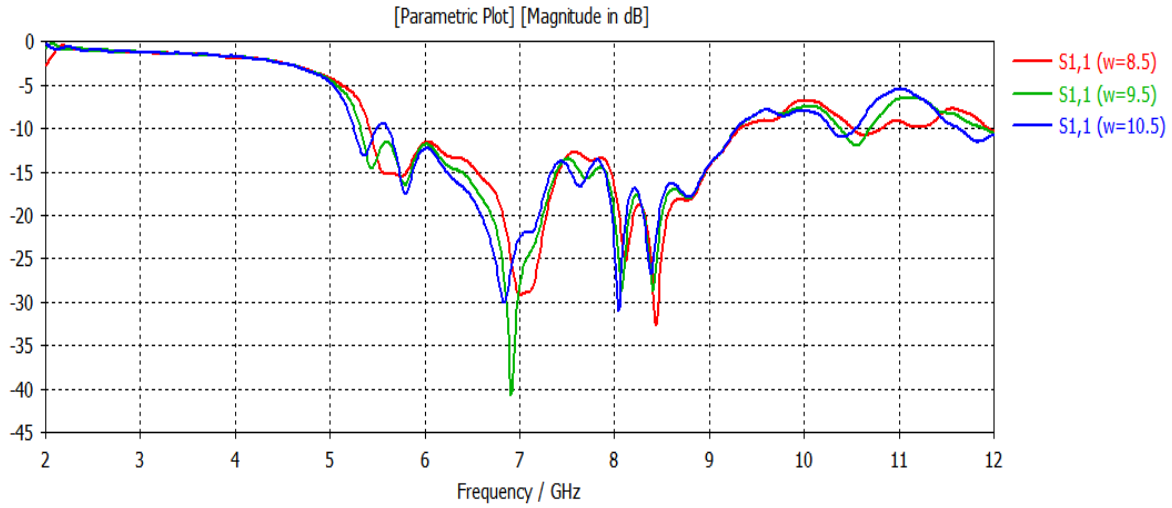

Figure 3.16 Comparison of S_{11} (dB) plot of the Proposed Antenna.

The Wg1 in ground plane is varied for three sample values as shown in Figure 3.16 to achieve the desired optimized antenna. It can be notice that at w=8.5mm, the band is right shifted with poor impedance matching. At w=9.5mm a wideband with better return loss value is obtained and at w=10.5mm the band is left shifted with poor impedance matching. Thus the best optimized value obtained from the given samples is at w=9.5mm.

3.4.3.2 Varying Lg2 in the Ground Plane

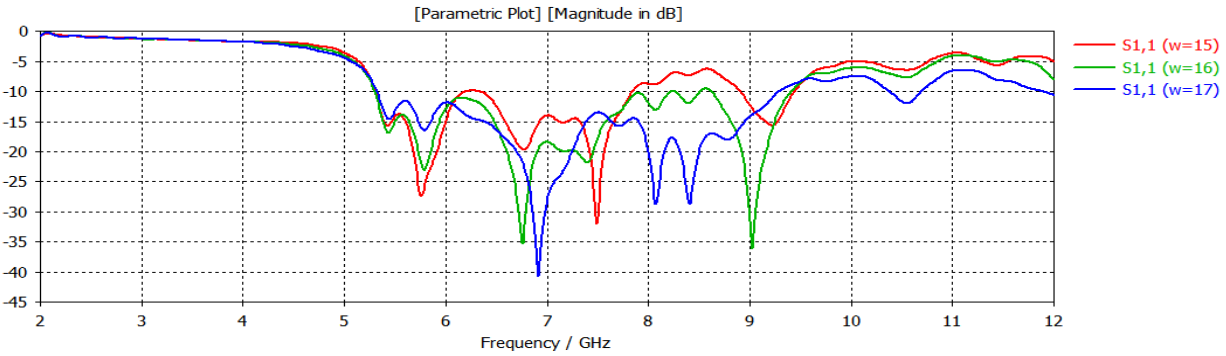

Figure 3.17 Comparison of S_{11}(dB) plot of the Simulated Antenna.

Figure 3.17 shows the variation of the length of slot in the ground plane for three sample values 15mm, 16mm and 17mm that result in shifting of resonant frequencies towards right or left. At w=17mm antenna is best matched to the standard impedance of 50ohms and this helps in exciting the entire band that is required for the intended UWB application and is therefore optimized one.

3.4.3.3 Effect of Varying width of stub with the feed line

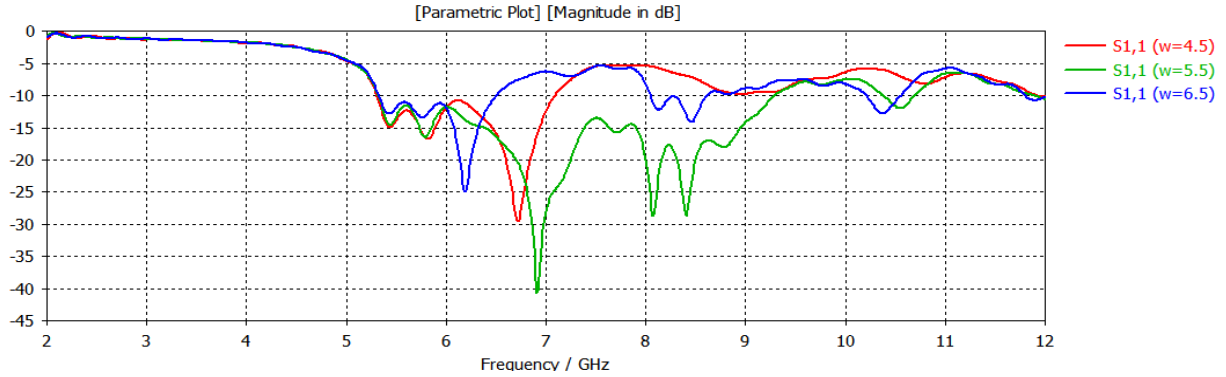

Figure 3.18 Comparison of S_{11} (dB) plot of the Simulated Antenna.

As illustrated in Figure 3.18, the variation in the width of the stub along x-axis results in the improved impedance bandwidth of the proposed antenna. The best optimized value is obtained at w=5.5mm and it is kept fixed for the final designing of the proposed antenna to achieve better impedance bandwidth.

3.4.4 Wireless Applications Covered by the Proposed Antenna

The proposed antenna operates in the frequency band from 5.3-9.28 GHz with bandwidth of 4180 MHz which makes the antenna suitable for the UWB operation (5.3-9.28 GHz), Radio Astronomy Band (5.01-5.03 GHz), IEEE 802.11a WLAN applications (5.15 to 5.825 GHz), STM band applications (6–6.17 GHz) and downlink X-band satellite communication (7.25 - 7.75 GHz).

3.5 DESIGN OF PLANAR COMPLEMENTRY BOWTIE APERTURE COUPLED ANTENNA FOR UWB APPLICATIONS

This subsection presents a planar complementary bowtie aperture coupled antenna to achieve UWB applications. The proposed antenna is simulated using CST MWS'14 for UWB applications. Various antenna design parameters such as tuning stub and slots in the ground plane are optimized to achieve desired antenna performance.

3.5.1 Antenna Design and Parameters

The proposed antenna is a aperture coupled two layer radiating structure of commercially available epoxy glass substrate (FR4 lossy) with a dielectric constant Ɛr=4.4, loss tangent of 0.0024 and a height of h=1.57mm for both layers of the antenna. The design process starts with two triangular generators joined at the apex. The partial ground lies between these two substrates. An equilateral triangle bowtie patch with side of 14.6mm for the zeroth iteration printed on the top of the substrate layer is shown in Figure 3.19(a). This bowtie fractal patch is modified at each iteration with triangular slots cut from it of reduced size compared to the original triangular patch size. It is observed that as the iteration order increases, the resonant frequency becomes lower than that obtained from the zeroth order of the iteration, thus allowing antenna to cover lower frequency bands for different applications without increase in the physical dimensions of the main bowtie antenna.

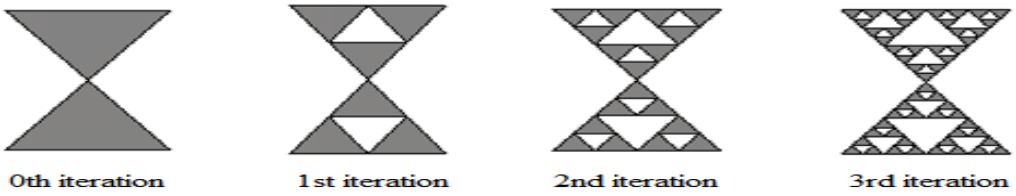

(a)

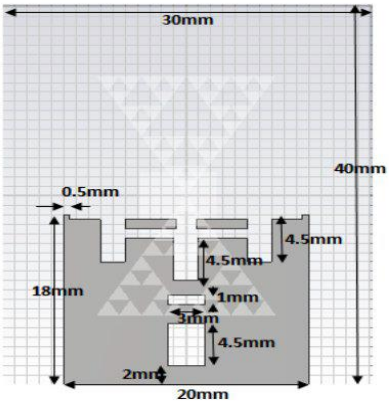

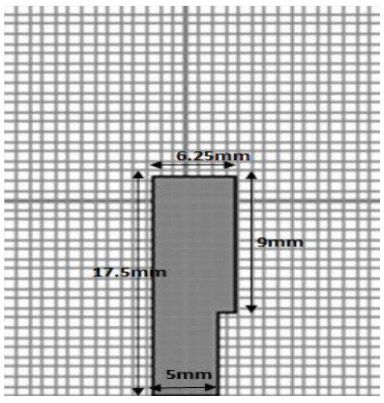

(b) (c)

Figure 3.19 Schematic diagram of Proposed Antenna (a) Various Level of Iteration (b) Ground Plane (c) Back View.

Figure 3.19(b) presents the middle view of the reduced ground plane with defected slots in it. The various slots in the ground plane help to achieve the better impedance bandwidth for the proposed antenna. Similarly Figure 3.19(c) presents the bottom view of the proposed antenna which consist of feed-line with a vertical tuning stub which further helps in obtaining the improved bandwidth for an UWB performance.

3.5.2 Simulation Results and Discussion

All the simulation results related to antenna designs were carried out using CST MWS version 2014. The patch, ground plane, feed-line, aperture and tuning stub were optimized for the desired results. The simulation results in terms of impedance bandwidth, gain, smith chart and surface current distribution are presented in the next subsections.

3.5.2.1 *Impedance bandwidth*

Figure 3.20 shows the comparative study of simulated S11 (dB) plot of the antenna on y-axis with respect to the frequency on x-axis. As 3rd iteration covers a wider band as compared to other iterations therefore it is considered as the final optimized one. The antenna is matched to 50ohms impedance at the drive point. The geometrical parameters of the antenna's ground plane and the feed-line are optimized to obtain an UWB of frequency range lying between 4.08-6.2 GHz. The antenna shows two resonant peaks at 4.8 GHz and 5.6 GHz with a peak return loss of - 17.82 dB and -19.98 dB.

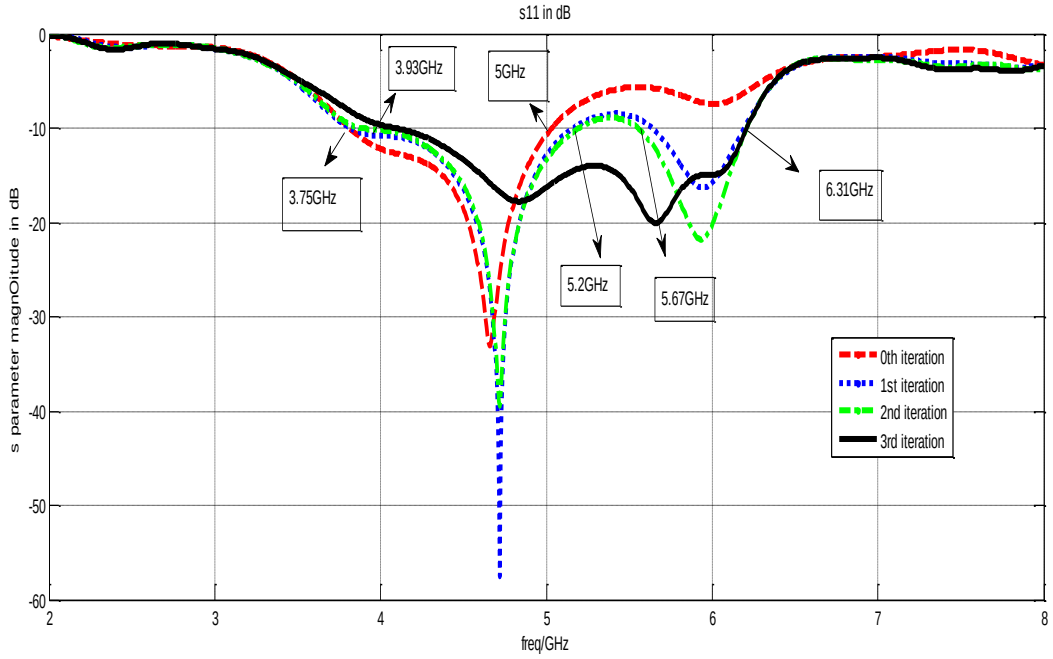

Figure 3.20 Simulated S_{11}(dB) plot of the Proposed Antenna.

3.5.2.2 Smith chart

Figure 3.21 shows the smith chart plot of the simulated bowtie fractal antenna to the second order of iteration. Markers show the resonant frequencies at 4.8 GHz and 5.6 GHz respectively of the optimized antenna.

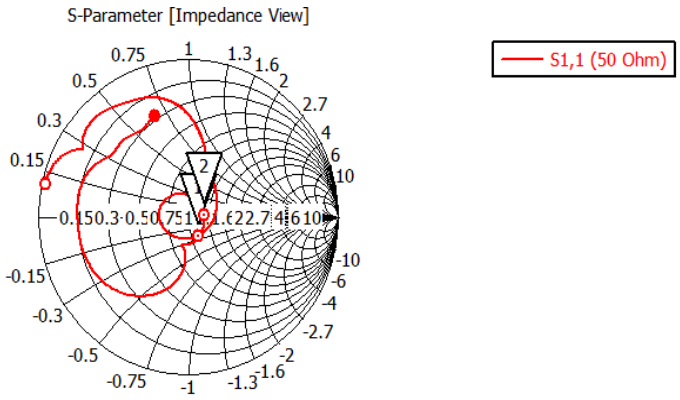

Figure 3.21 Smith chart of the Simulated Antenna.

3.5.2.3 Gain

Figure 3.22 shows the simulated gain plot versus frequency of the proposed antenna. The maximum achievable gain for the proposed antenna is 3.64 dB at a resonant frequency of 5.3 GHz.

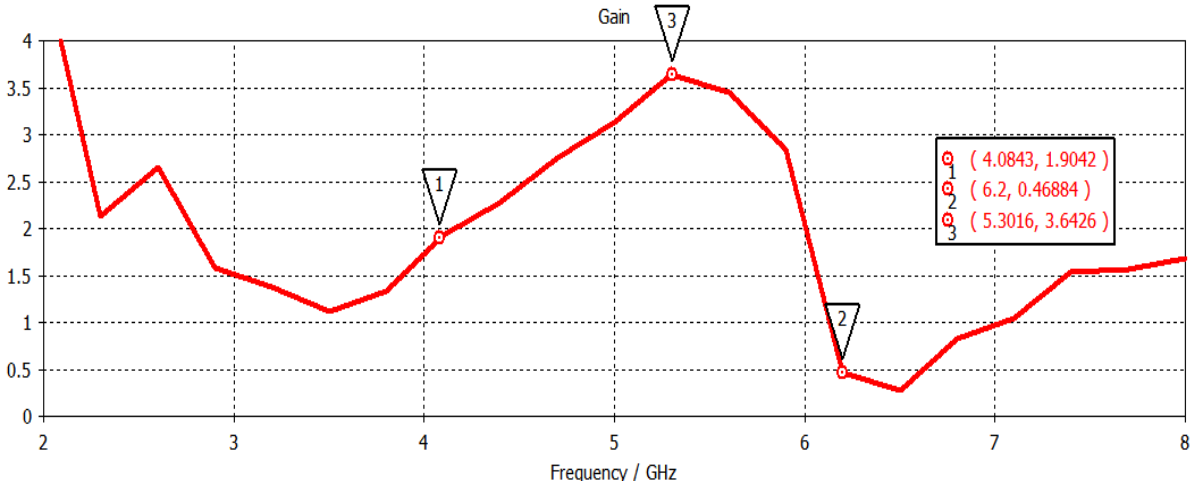

Figure 3.22 Simulated S_{11} (dB) plot of the Proposed Antenna

Figure 3.23(a) demonstrates the 3D view of gain at a resonant frequency of 5.3 GHz. Figure 3.23(b-c) shows polar plot for peak gain of the proposed UWB antenna for elevation and azimuthal plane at 5.3GHz frequency. As shown in Figure 3.23(b), the major lobe is directed at an angle of 1.0 degrees with magnitude of 1.79dB and half power beam width of 148.8degrees. The elevation pattern shows a directional radiation pattern along the elevation plane. The antenna is directional along the azimuthal plane also that can be examined from Figure 3.23(c).

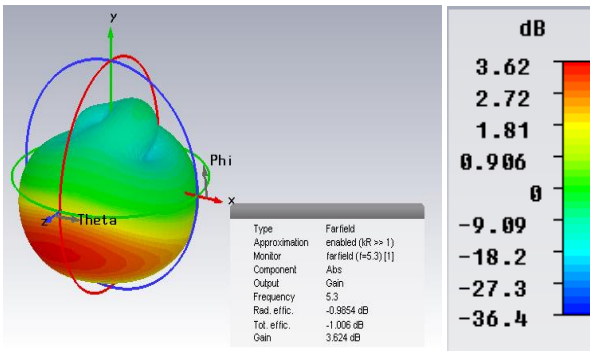

(a)

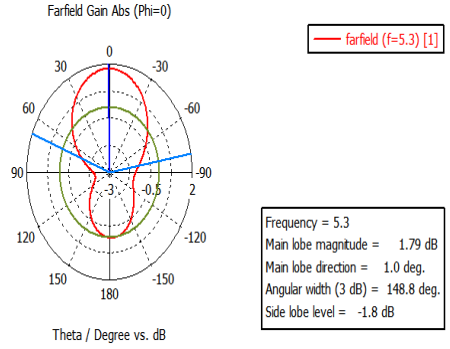

(b)

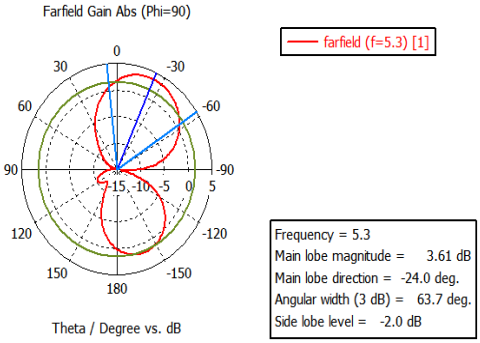

(c)

Figure 3.23 Proposed Antenna (a) 3D peak Gain plot at 5.3 GHz frequency (b) Polar Gain Plot for Elevation Plane at 5.3 GHz (C) Polar Gain Plot for Azimuthal Plane at 5.3 GHz.

3.5.2.4 Surface current distribution

Figure 3.24(a-f) shows the surface current distribution on the various layers of antenna for resonant frequencies 4.8 GHz and 5.6 GHz when antenna is energized using an aperture coupled feeding. It is demonstrated from the Figure 3.24(a) that the maximum magnitude of the current flows at the lower part of the patch for resonant frequency at 4.8 GHz. Figure 3.24(b) shows that the current is flowing through the middle slot that is embedded in the ground plane at 4.8 GHz. Figure 3.24(c) shows the current distribution at the feedline for the resonant frequency 4.8 GHz. Figure 3.24(d) illustrates the current distribution on patch at resonant frequency 5.6 GHz. This figure indicates that the maximum current flows through the boundaries of 2^{nd} iterated triangular slots in the patch. Figure 3.24(e) demonstrates that the current flows through all the slots in the ground plane for the resonant frequency at 5.1 GHz. Figure 3.24(f) shows that the maximum magnitude of current is at the lower part of the feedline for the resonant frequency at 5.6 GHz. Thus Figure 3.24(a-f) helps in explaining that lower side of patch is responsible for exciting 4.8 GHz frequency. The slots in ground plane are responsible for resonant frequency of 5.6 GHz and feedline is responsible for exciting both the lower as well as higher resonating band at 4.8 GHz and 5.6 GHz respectively.

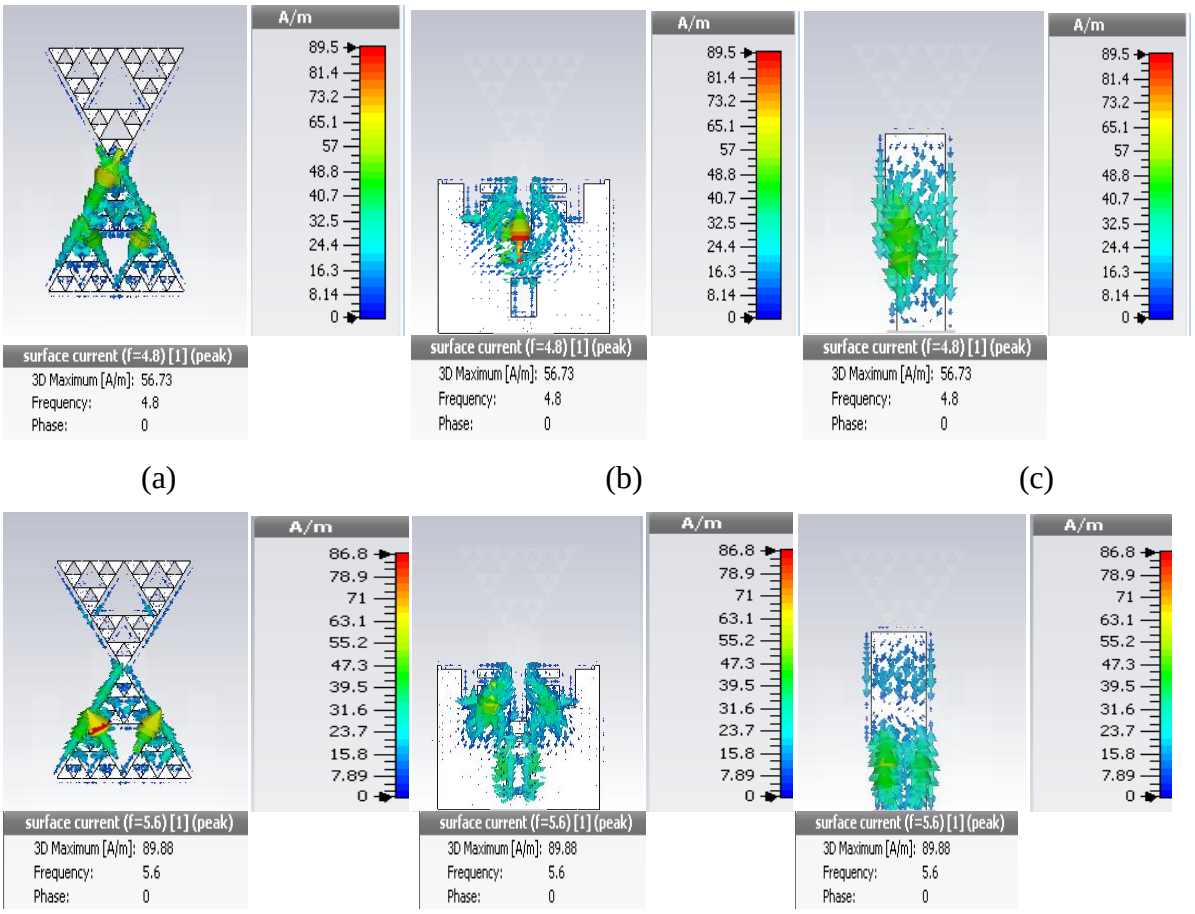

Figure 3.24 Surface current distribution of the proposed antenna at resonating frequencies (a-c) 4.8 GHz (d-f) 5.6GHz.

3.5.3 Parametric Variations of the Proposed Antenna

This section presents the parametric variations of the proposed antenna that are carried out in order to achieve the desired results for various wireless applications.

3.5.3.1 Varying length of the stub in the feed-line

As demonstrated in Figure 3.25, the variation in the length of the stub along y-axis results in the improved impedance bandwidth of the proposed antenna. The best optimized value with wider bandwidth and improved impedance matching is obtained for sample value of w=19mm and it is kept fixed for the final optimization of the proposed antenna.

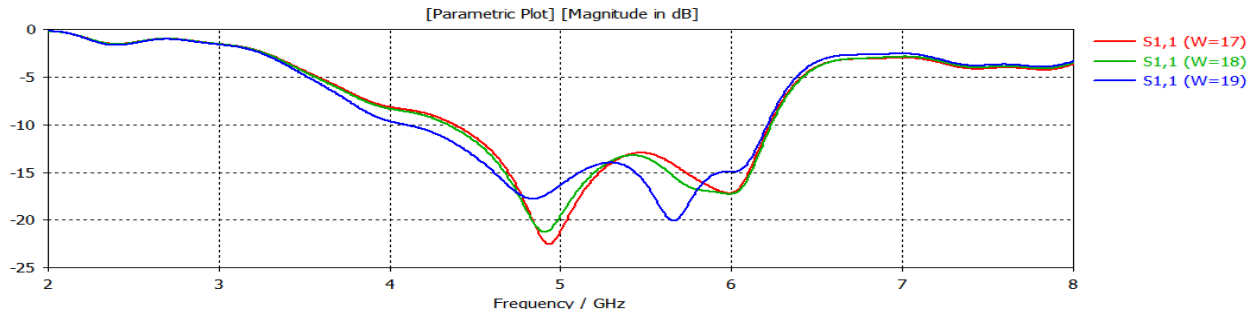

Figure 3.25 Comparison of Simulated S_{11} (dB) plot of the Antenna by varying the length of the stub in the feed-line.

3.5.3.2 Varying length of the feed-line

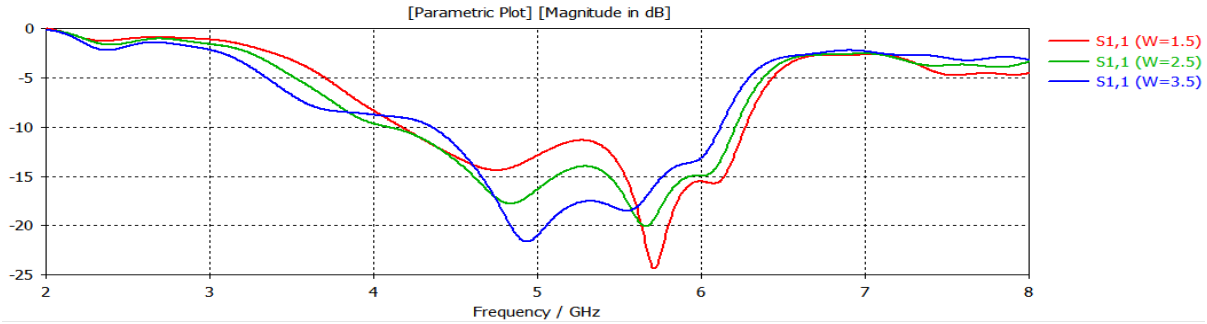

Figure 3.26 Comparison of Simulated S_{11} (dB) plot of the antenna by varying the length of the feed-line.

Figure 3.26 shows the S_{11} (dB) values for variation of the length of the feedline for three sample value of 1.5mm, 2.5mm and 3.5mm respectively. For w=1.5mm, a right shifted band with poor impedance bandwidth is obtained. For w=2.5mm, a widerband with better impedance matching is achieved whereas for w=3.5mm, a left shifted narrow band is achieved. Therefore the best optimized value out of three samples is w=2.5mm and is kept fixed for designing the proposed antenna.

3.5.4 Wireless Applications Covered by Proposed Antenna

The antenna is iterated to 3rd level which helps it to exhibit a frequency band of 3.7-5.4 GHz and thus shows an UWB operation (3.71-10.6 GHz), INSAT (Indian National Satellite systems) (4.5-4.8 GHz), WLAN applications (5.15-5.825 GHz), Radio Astronomy applications (5.01-5.03 GHz). The maximum achievable gain for the proposed antenna is 3.64 dB at 5.3 GHz frequency.

3.6 DESIGN OF CUP SHAPED MICROSTRIP PATCH ANTENNA FOR UWB APPLICATIONS

This section presents the designing and simulation of a cup shaped micro-strip patch antenna with reduced ground plane for UWB applications using CST MWS V'14. The simulation results are analyzed in terms of return loss, bandwidth, smith chart, gain and surface current distribution. The parametric study of various antenna design parameters are carried out to obtain optimum UWB operation.

3.6.1 Antenna Design and Specifications

Figure 3.27(a) shows a microstrip line fed cup shaped antenna designed on a FR4 substrate with h=1.57 mm, Ɛr=4.4 and loss tangent loss of 0.0024. the antenna is made on FR4 subsatre with dimensions of 24 mm×20 mm×1.6 mm. The dimensions of various antenna design parameters such as patch, ground and substrate are calculated using transmission line model

equations discussed in section 3.2. The antenna is composed of microstrip feed line, L-shaped ground plane and rectangular shaped patched. L-shaped ground structure is achieved by modifying rectangular ground plane and eliminating the square-shaped slot from it. The rectangular radiator is modified by placing a semi- circular slot of radius Rp at the upper edge and an equilateral triangular slot of side length Wt at the centre of the radiating element to form a cup-shaped slot as shown in Figure 3.27(a). On the reverse of the substrate, the radiating patch fed with micro-strip line of length Lf is placed. The optimized dimensions of various antenna design parameters are specified in Table 3.3.

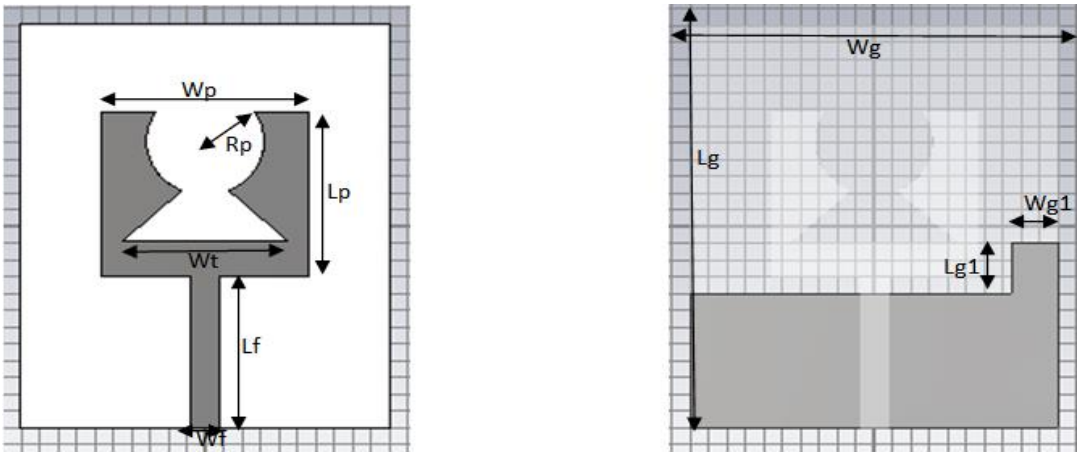

(a) (b)

Figure 3.27 Proposed Antenna Design (a) Top View (b) Bottom View.

Parameters	**Dimensions**
Wp	11.2mm
Lp	9.8mm
Lf	9mm
Wf	1.6mm
Wg	20mm
Lg	24mm
Wg1	2.5mm
Lg1	3mm
Rp	3.2mm
Wt	9mm

Table 3.3 Optimized dimensions of the Proposed Antenna.

3.6.2 Simulation Results and Discussion

CST MWS V' 2014 is used for designing and simulating the results of antenna parameters such as return loss, smith chart, VSWR, gain and current distribution which are discussed below.

3.6.2.1 Impedance Bandwidth

Figure 3.28 shows the simulated return loss plot as the function of frequency. For maximum power transfer to the antenna return loss should be as small as possible in the negative range (below -10dB). The proposed antenna covers the frequency range from 4.9-25.9 GHz with bandwidth of 21 GHz. The peak return loss of -40.27 dB is obtained at resonant frequency of 14.4 GHz.

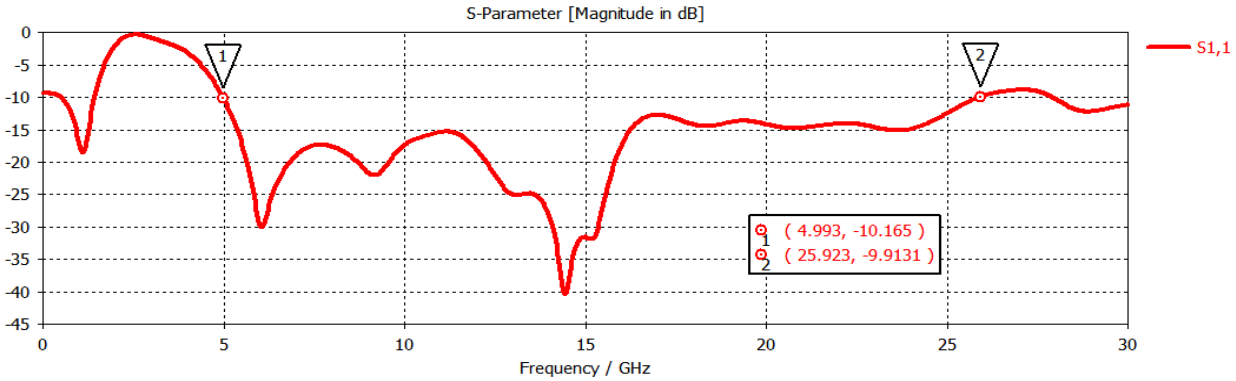

Figure 3.28 Simulated S_{11} (dB) plot of the Proposed Antenna.

3.6.2.2 Smith chart

The smith chart for the proposed antenna is shown in Figure 3.29. For proper impedance matching, the locus of the smith chart must pass through its center. It provides an impedance of 50 ohm which is makes the proposed antenna suitable for practical applications. Markers show the resonant frequencies at 6.06 GHz and 14.43 GHz respectively of the optimized antenna.

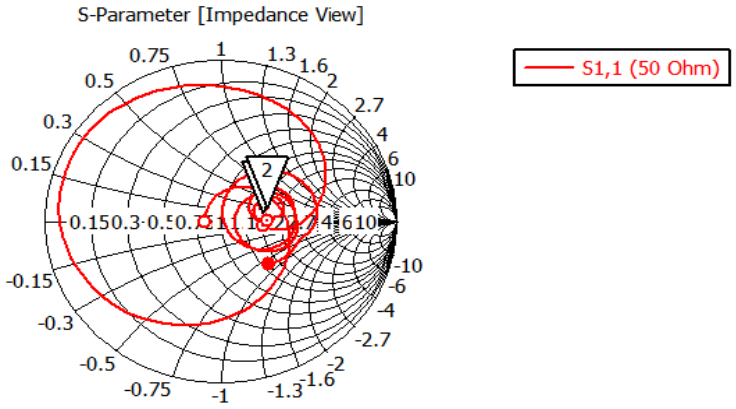

Figure 3.29 Smith chart of the Proposed Antenna.

3.6.2.3 Gain

Figure 3.30 shows the simulated broadband gain plot versus frequency of the proposed antenna. The maximum achievable peak gain for the proposed antenna is 4.78 dB at 16.48 GHz resonant frequency

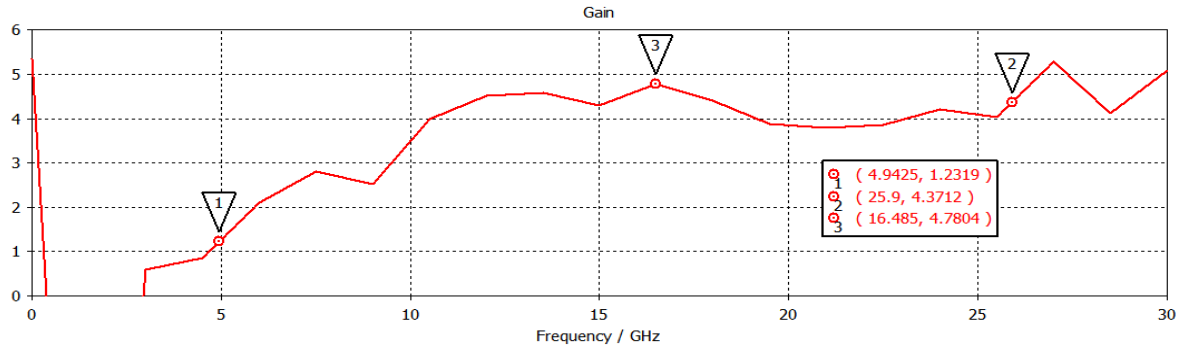

Figure 3.30 Broadband Gain of the Proposed Antenna.

Figure 3.31(a) demonstrates the 3D view gain of the proposed UWB antenna at a frequency of 5.16 GHz. Figure 3.31(b-c) shows polar plot of proposed antenna for elevation plane and azimuthal plane respectively. As shown in Figure 3.31(b), the major lobe is directed at an angle of 32 degrees with magnitude of 2.48 dB and half power beam width of 55.1degrees. The elevation pattern shows a directional radiation pattern along the elevation plane. The proposed antenna is also directional along the azimuthal plane that can be examined from Figure 3.31(c)

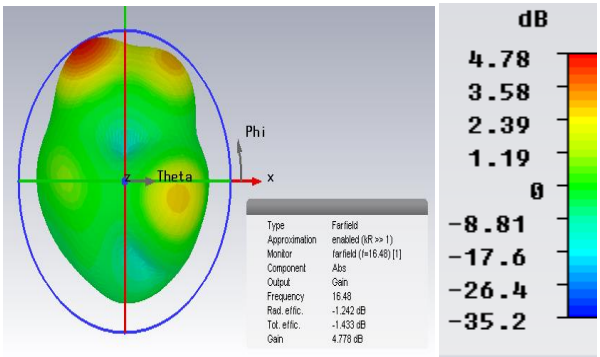

(a)

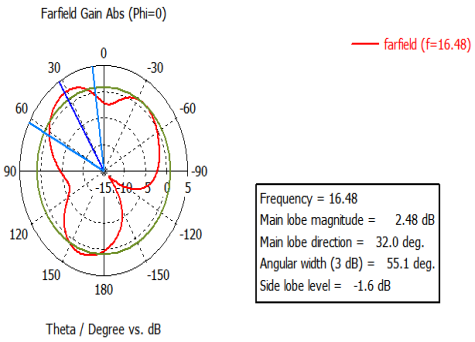

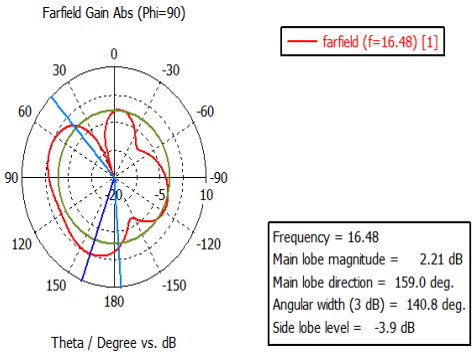

(b) (c)

Figure 3.31 Proposed antenna (a) 3D Gain at 16.48 GHz frequency (b) Polar plot of antenna for elevation plane (c) Polar plot of antenna for Azimuthal Plane.

3.6.2.4 Surface current distribution

Figure 3.32(a-d) shows the surface current distribution on the patch and ground plane of antenna for resonant frequencies 6.06 GHz and 14.43 GHz when antenna is excited using

microstrip feedline in the software. It is demonstrated from Figure 3.32(a) that the maximum current flows through the lower edges of the cup shaped patch and through the overall boundary of microstrip feedline for resonant frequency 6.06 GHz. Figure 3.32(b) illustrates the current flows through the overall dimension of the ground plane at 6.06 GHz operating frequency but the maximum magnitude of current is seen at the one end of extended ground plane. Figure 3.32(c) shows the maximum intensity of the current flows through the entire patch and feedline but the maximum current distribution is seen at the lower edges of cup shaped patch and on the upper boundary of the feedline at resonant frequency 14.43 GHz. Similarly Figure 3.32(d) shows that the maximum magnitude of the current flows through the one end of the extended ground plane at 14.43 GHz resonant frequency.

Hence it can be concluded that lower edges of triangular slots in patch and feedline are responsible for resonating lower resonant frequency of 6.06 GHz and partial ground plane is responsible for exciting higher resonant frequency of 14.43 GHz.

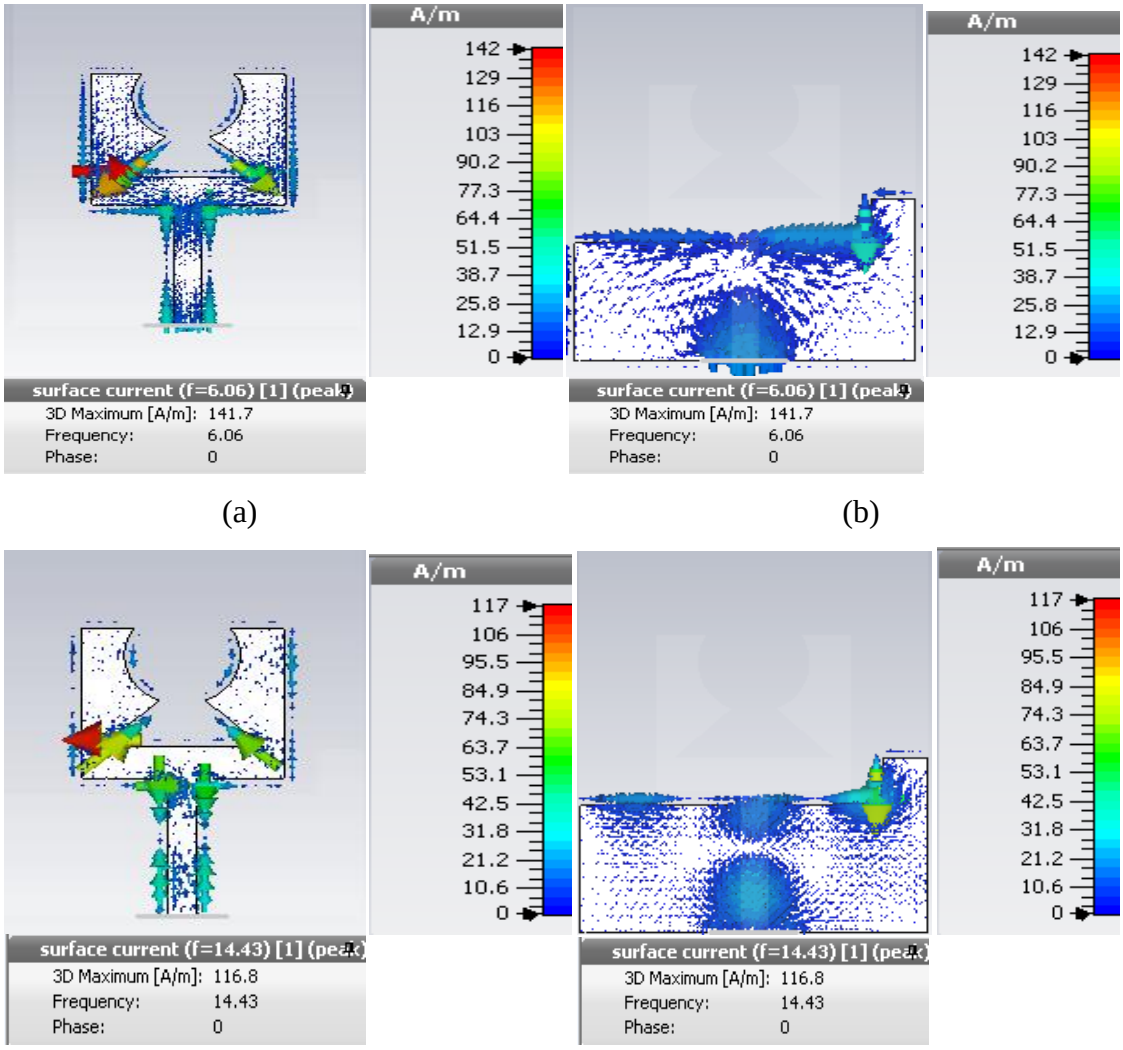

Figure 3.32 Surface current distribution of the proposed antenna at resonating frequencies (a-b) 6.06 GHz (c-d) 14.43 GHz.

3.6.3 Parametric Variations of the Antenna Parameters

The major goal of the proposed antenna design is to achieve miniaturization and ultra wideband characteristics with good impedance matching performance. In this section, various antenna design parameters such as dimension of ground plane, slots in the patch are investigated to enhance the bandwidth of antenna. The best optimized dimensions for the antenna parameters are chosen to achieve the desired performance from the proposed antenna.

3.6.3.1 Varying L-shaped ground structure

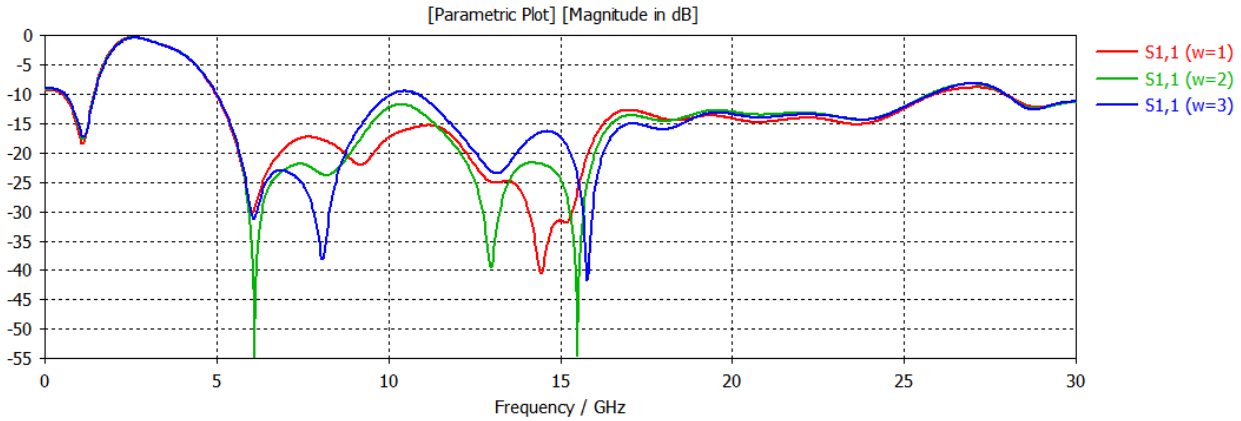

Figure 3.33 Comparison of S_{11} (dB) parameters by varying the length of L-shaped ground structure.

As illustrated in Figure 3.33, the length of L-shaped ground plane is varied for three samples values. For w=1mm a wider bandwidth with good impedance matching is achieved whereas at w=2mm and w=3mm a right or left shifted band with poor impedance matching is obtained. Therefore the optimized value for the length of the L-shaped slot obtained is w=1mm.

3.6.3.2 Varying width of the feed-line

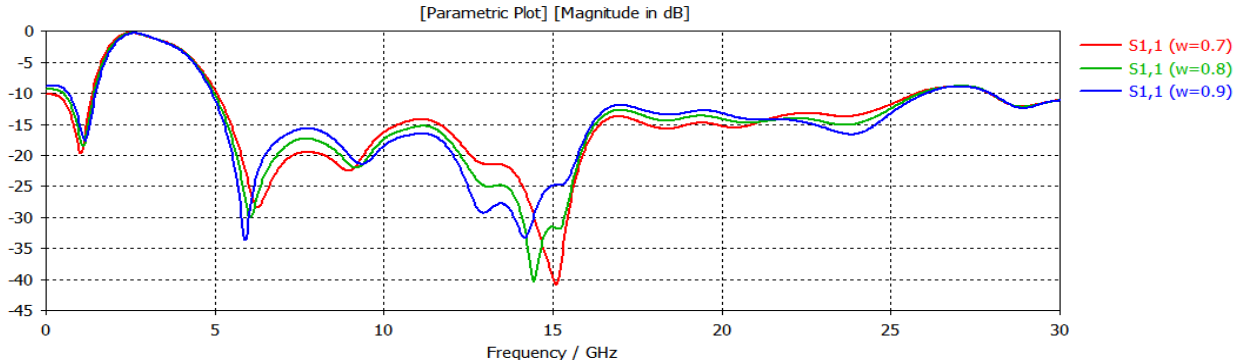

Figure 3.34 Comparison of S_{11} (dB) parameters by varying width of the feed-line.

The width of the feed-line for the sample values of 0.7mm, 0.8mm and 0.9mm is varied to obtain the optimized results for the proposed antenna as shown in Figure 3.34. The feed

width of 0.8mm covers the largest bandwidth of 21 GHz and efficiently resonates at 6.06 GHz and 14.43 GHz frequencies and is therefore selected as the optimized one.

3.6.4 Wireless Applications Covered by the Proposed Antenna

The proposed antenna covers X band(2-8 GHz), Ku band(8-12 GHz) and K band(12-18 GHz). This frequency band makes the antenna suitable for the UWB applications(4.9-25.9 GHz), Radio Astronomy Band(5.01-5.03GHz), INSAT (Indian National Satellite systems) (4.8-4.10 GHz), WLAN applications(5.15-5.535 GHz, 5.725-5.825 GHz), downlink X-band satellite communication (7.25- 7.75 GHz), Amateur Satellite operations(10.45-10.5 GHz), marine time radar(13.25-14 GHz), radio determination applications(15-18.8 GHz).

3.7 CHAPTER CONCLUSION

This chapter presents the design and simulation results of four UWB antennas. A plus shape fractal that covers the frequency band ranging from 3.9-4.0 GHz, 4.8-5.0 GHz, 6.1-6.4 GHz, 6.9-11.3 GHz with adequate bandwidth of 100 MHz, 200 MHz, 300 MHz and 4400 MHz respectively is presented. Next a Koch fractal aperture coupled antenna that covers the frequency band ranging from 5.3-9.2 GHz with adequate bandwidth of 3900 MHz resonating at 6.9 GHz, 8.0 GHz and 8.4 GHz respectively is presented. A complementary bowtie fractal antenna that covers the frequency range lying between 4.08-6.2 GHz is presented. The antenna shows two resonant peaks at 3.9 GHz and 5.1 GHz with a peak return loss of -17.82 dB and -19.98 dB respectively. Next is a cup shaped microstrip line fed antenna that covers the frequency range from 4.9-25.9 GHz with bandwidth of 21 GHz. The peak return loss of -40.27 dB is obtained at resonant frequency of 14.4 GHz is presented.

CHAPTER-4
FABRICATION AND EXPERIMENTALTESTING OF PROPOSED UWB ANTENNAS

4.1 INTRODUCTION

This chapter presents the fabrication of the proposed UWB antenna mentioned in chapter-3. The fabrication and testing of antenna is carried out to check the applicably of antenna. The antenna was fabricated on an FR4 substrate and Photolithography (wet etching) process was used for the fabrication of antenna. The return loss was measured using Agilent's vector network analyzer (VNA) model no E5063A whose operating frequency range is from 0 to 20 GHz.

4.2 FLOWCHART FOR THE FABRICATION PROCEDURE OF ANTENNA

This section describes the fabrication procedure of the Fractal antenna using Aperture Coupled feeding technique. The flowchart gives the complete fabrication steps of antenna in sequential manner and is given below:

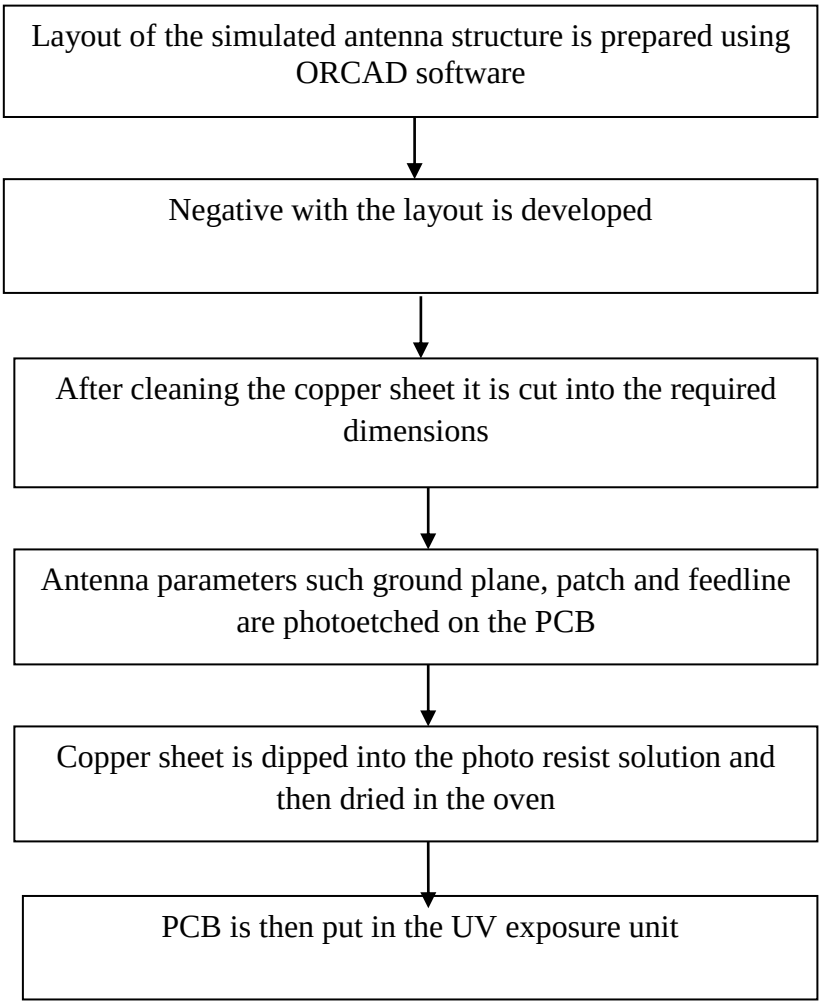

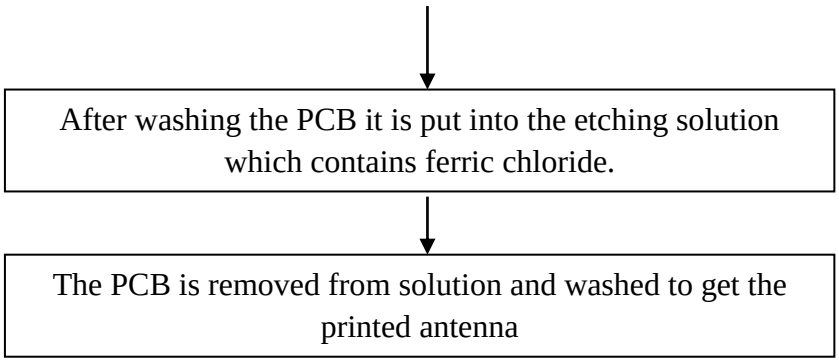

Figure 4.1 Flow Chart for the Fabrication Procedure of the Proposed Antenna.

4.3 TESTING OF FRACTAL ANTENNA

Figure 4.2 shows Agilent's vector network analyzer (VNA) model no E5063A for testing the antenna, whose operating frequency range is from 0 to 20 GHz.

Figure 4.2: Vector Network Analyzer for testing.

4.4 FABRICATION OF A PLUS SHAPED CARPET FRACTAL ANTENNA

The antenna was fabricated using the procedure mentioned in flow chart. Figure 4.3(a) shows the view of top layer of antenna. Figure 4.3(b) shows the view of ground plane for the carpet fractal and Figure 4.3(c) shows the bottom view of the ground layer with feedline.

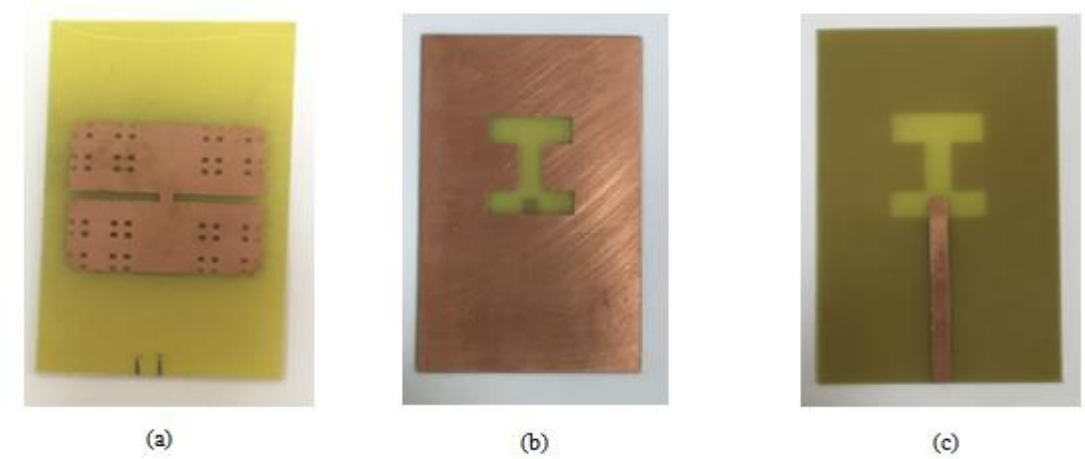

Figure 4.3 Photograph of the Fabricated Antenna (a) Front View of the Fabricated Antenna (b) I-shaped ground plane structure of the fabricated antenna (c) Bottom View of the Fabricated Antenna.

4.4.1 Comparison of Simulated and Measured Results of the Proposed Carpet Fractal Antenna

Figure 4.4 shows the comparison of simulated and measured results of the proposed antenna. The measured results show the first resonant frequency at 5.3GHz covering the bandwidth of 250MHz ranging from 5.2-5.45 GHz, second resonant frequency at 5.75GHz covering the bandwidth of 200MHz ranging from 5.65-5.85GHz, third resonant frequency at 6.7GHz covering the bandwidth of 400MHz ranging from 6.5-6.9 GHz and fourth resonant frequency at 9.2 GHz covering the bandwidth of 3100MHz ranging from 7.2-10.3 GHz. While the simulated results show its first resonant frequency at 4.02 GHz covering the bandwidth of 150MHz ranging from 4-4.15GHz, second resonant frequency at 6.25 GHz covering the bandwidth of 350MHz ranging from 6.1-6.4GHz, third resonant frequency at 7.5GHz covering the bandwidth of 4850MHz ranging from 6.95-11.8GHz. It can be seen that the measured results have a close resemblance with the simulated results and are little shifted towards right. A 75% matching is seen in the two results. This shift in the results can be attributed to the errors introduced during fabrication process and testing of antenna because of misalignment of the two layers of substrate. The measured results show that the antenna is practically suitable for wireless applications such as WLAN, WiMAX, Wi-Fi, UWB, Satellite communication, Radar communication.

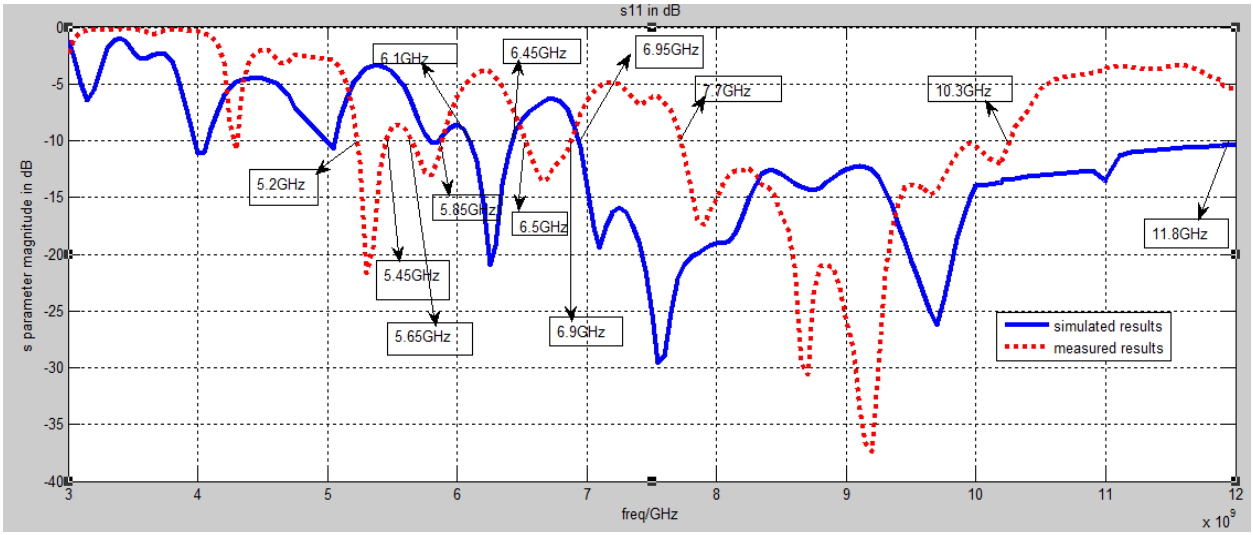

Figure 4.4 Comparison of Simulated and Measured results of the Proposed Antenna.

Parameters	Simulated Results	Measured Results
Resonant frequency	4.01 GHz, 6.25 GHz and 7.5 GHz	5.3 GHz, 5.75 GHz, 6.7GHz and 9.2 GHz
Impedance bandwidth	150 MHz, 350 MHz and 4850 MHz	250 MHz, 200 MHz, 400 MHz and 3100 MHz

Return loss at resonant frequency	-12.45 dB, -21.66 dB and -28.91 Db	-22.35 dB, -13.94 dB, -14.27 dB and -37.93 dB
Applications covered	C band, X band,WLAN, WIMAX, UWB, Wifi	C band, X band, WLAN, WIMAX, UWB, Wifi

Table 4.1 Comparison of Simulated and Measured Results of the Proposed Antenna.

4.5 FABRICATION OF A BOWTIE APERTURE COUPLED FRACTAL ANTENNA

The bowtie shaped fractal antenna is fabricated using the process mentioned in flowchart. Figure 4.5(a) shows the top view of antenna. Figure 4.5(b) shows the ground layer and Figure 4.5(c) shows the bottom view of the ground layer with feedline.

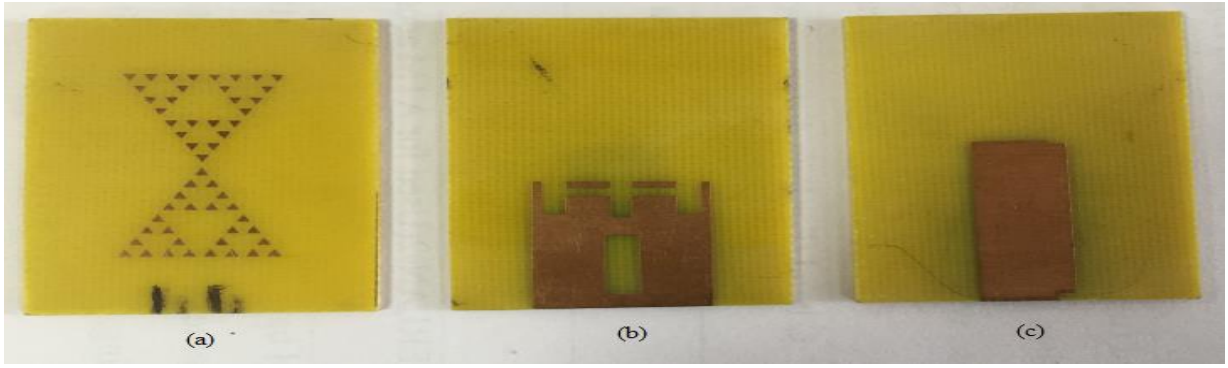

Figure 4.5 Photograph of the fabricated antenna (a) Front view of the fabricated antenna (b) Reduced ground plane structure of the fabricated antenna (c) Back view of the fabricated antenna.

4.5.1 Comparison of Simulated and Measured Results of the Proposed Antenna

Figure 4.8 shows the comparison of simulated and measured results of the proposed antenna. The measured results show the first resonant frequency at 2.08 GHz covering the bandwidth of 110 MHz ranging from 2.75-2.86 GHz, second resonant frequency at 5.6 GHz covering the bandwidth of 940 MHz ranging from 4.88-5.82 GHz While the simulated results covers the frequency range from 4.08-6.2 GHz with impedance bandwidth of 2250 MHz. The shift in the measured results can be attributed to the errors introduced during fabrication process and testing of antenna because of misalignment of the two layers of substrate.

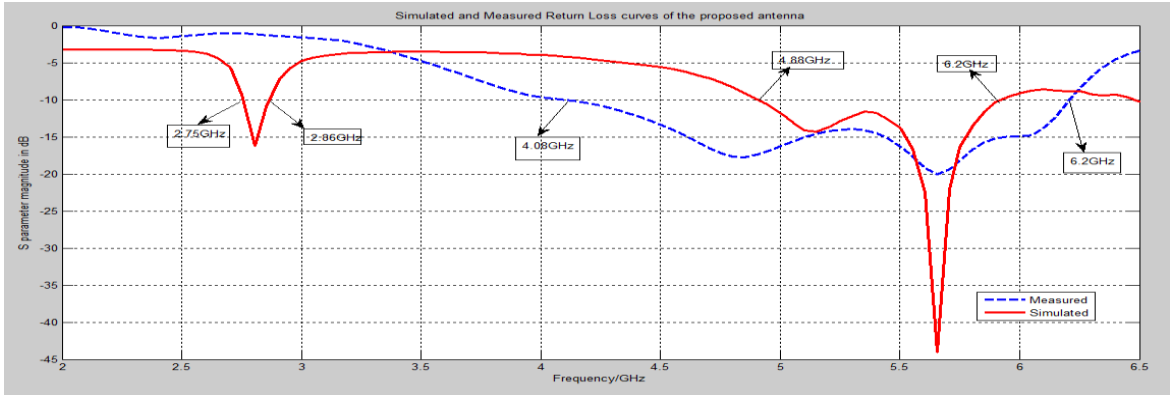

Figure 4.6 Comparison of simulated and measured results of the Proposed Antenna.

Parameters	Simulated Results	Measured Results
Resonant frequency	4.8 GHz and 5.6 GHz	2.08 GHz and 5.62 GHz
Impedance bandwidth	2250 MHz	110 MHz and 940 MHz
Return loss at resonant frequency	-17.82 dB and -19.81dB	-17.01 dB and -44.12 dB
Applications covered	C band, X band,WLAN, WiMAX, UWB, Wifi, amateur radio	C band, X band, WLAN, WiMAX, UWB, Wifi, amateur radio

Table 4.2 Comparison of Simulated and Measured Results of the Proposed Antenna.

Table 4.2 represents the comparative study of simulated and measured results of proposed bowtie fractal antenna. The measured results show the resonant frequencies at 2.08 GHz and 5.62 GHz with impedance bandwidth of 110 MHz and 940 MHz respectively whereas simulated results show the resonant frequencies at 4.86 GHz and 5.62 GHz with impedance bandwidth of 2250 MHz.

4.6 CONCLUSION

This chapter presents the fabrication and experimental testing of two UWB antennas that were designed and simulated in chapter-3. It is seen that the simulated and measured results closely match allowing the antenna to be practically suitable for WiMAX, UWB, Wi-Fi, satellite communication, military systems and radar communication applications.

CHAPTER 5
CONCLUSION AND FUTURE SCOPE

5.1 CONCLUSION

This thesis report presents three configurations for Fractal MPA with Aperture coupled feeding arrangement and one as cup shaped MPA covering a broadband for every wireless application. The three Fractal MPAs designed are Plus shaped, Koch and Bowtie using aperture coupled feeding technique. For these antennas various antenna characteristics such as return loss, gain, bandwidth, smith chart, surface current distribution and operating frequencies are studied. The impact of physical parameters on the antenna parameters are additionally contemplated in this report.

- Chapter 1 starts with overview of fractal antennas and their origination in history. The research gaps and thesis objectives are presented in this chapter.
- Chapter 2 presents the literature review done in this regard.
- Chapter 3 starts with the study of the multi band antenna covering wireless applications using aperture coupled feeding technique. The Plus shaped patch with three level iteration helps in enhancing the outcomes, bandwidth, gives the multiple frequency bands. The length, width and the position of the slots are varied in order to acquire the coveted results for the proposed antenna. The designed antenna shows its first resonant frequency at 4.01 GHz covering the bandwidth of 180 MHz ranging from 3.9-4.08 GHz, second resonant frequency at 6.2 GHz covering the bandwidth of 300 MHz ranging from 6.1-6.4 GHz, third resonant frequency at 7.5 GHz and 9.6 GHz covering the bandwidth of 4460 MHz ranging from 6.93-11.39 GHz.
    - The next work presents the geometry of the proposed Aperture coupled-fed Koch fractal based slot antenna. The basic geometry of the slot is an equilateral triangle of side ‘a’ on which repeated iterations leads to the Koch snowflake structure. The proposed antenna resonates at 6.9 GHz, 8.0 GHz and 8.4 GHz frequencies with the impedance bandwidth of 3900 MHz covering the frequency band of 5.3- 9.2 GHz. The operating frequency covers the bandwidth of 53.7% which exceeds the required UWB range.
    - The next work deals with the designing of a planar complementary bowtie aperture coupled antenna for UWB applications. Various antenna design parameters such as tuning stub and slots in the ground plane are optimized to achieve desired results for the proposed antenna. This bowtie fractal patch is

modified at each iteration with reduced size compared to the original triangular patch size. This antenna resonates at 4.8 GHz and 5.6 GHz frequencies.

- The next work represents the designing and simulation of a cup shaped microstrip patch antenna with reduced ground plane for UWB applications. The dimensions of various antenna design parameters such as patch, ground and substrate are calculated using transmission line model. The proposed antenna covers the frequency range from 4.9-25.9 GHz with bandwidth of 21 GHz. The peak return loss of -40.27 dB is obtained at resonant frequency of 14.4 GHz. The proposed antenna covers X band (2-8 GHz), ku band (8-12 GHz) and k band (12-18 GHz). This frequency band makes the antenna suitable for the UWB applications (4.9-25.9 GHz).

➢ In chapter 4, two of the four the antennas designed and simulated in chapter 3 are fabricated and tested. The measured results are quite matching as compared to the simulated ones. In plus shaped fractal antenna the resonance shifted from 4.02 GHz, 6.25 GHz and 7.5 GHz to 5.3 GHz, 5.75 GHz, 6.7 GHz and 9.2 GHz. Further the variation in bandwidth is also noticed from 150 MHz, 350 MHz and 4850 MHz to 250 MHz, 200 MHz, 400 MHz and 3100 MHz. Similarly in bowtie aperture coupled antenna the resonance shifted from 4.86 GHz and 5.62 GHz to 3.92 GHz, 6.27 GHz and 6.88 GHz and the variation in bandwidth is noticed from 2250 MHz to 100 MHz, 200 MHz and 350 MHz. Both the fabricated and simulated antennas have find their applications in the field of C band, X band, WLAN, WiMAX, UWB and Wi-Fi.

Table 5.1 represents the comparison of all simulated and measured results of the proposed antenna in terms of resonant frequency, return loss, impedance bandwidth and gain of antenna.

Design	**Simulated Resonant Frequency (GHz)**	**Measured Resonant Frequency (GHz)**	**Simulated Return Loss (dB)**	**Measured Return Loss (Db)**	**Simulated Impedance Bandwidth (MHz)**	**Measured Impedance Bandwidth (MHz)**	**Simulated Gain (dB)**
Plus Shaped Fractal Antenna	4.01, 6.25 and 7.5	5.3, 5.75, 6.75 and 9.2	-12.45, -21.66 and -28.91	-22.35, -13.94, -14.27 and -37.93	180, 300 and 4460	250, 200, 400 and 3100	3.99
Koch Aperture Coupled Fractal Antenna	6.9, 8.0 and 8.4	-	-40.01, -27.82 and -27.64	-	3900	-	4.5

Bowtie Fractal Antenna	4.8 and 5.6	2.08 and 5.62	-17.82 and -20.01	-17.01 and -44.12	2250	110 and 940	3.64
Cup Shaped Microstrip Antenna	6.06 and 14.43	-	-29.99 and -40.27	-	21000	-	4.78

Table 5.1 Concluded Simulated and Measured Results of all the Designs.

5.2 FUTURE SCOPE

As the zone of fractal antenna engineering research is still in its early stages, there are numerous potential outcomes for future work on this topic. Number of fractal geometries exists that have desirable antenna characteristic. Thus other type of fractal structures can be studied for future work that can applicable in various antenna applications. A new pattern of fractal can be developed for antenna arrays. Fractal antennas can be studied in various areas such as in expanding wireless market. The polarizations of these antennas need to be studied for such applications. A lower covered area of resonant loop antennas is another advantage of fractal antennas. This results in lower cross sections of antenna. Further, fractal structures can also be used along with microstrip antennas for application in various wireless communication fields. Some such work that can be performed on proposed technique is mentioned below:

- Antennas using other fractal geometries like V-Koch, Sierpinski gasket, and Multi-band fractal antenna can be designed.
- Some preliminary studies on Sierpinski fractal loop antenna have been undertaken. This can be further characterized and also antenna can be optimized using evolutionary techniques such as MOPSO, Genetic Algorithms.
- CPW feed can be optimized with changing the shape of ground plane rather than perturbing the geometry itself.
- Stacked fractal antenna Engineering is another field that can be worked upon future.

Meta-materials can also be used to deign antennas: A meta-materials are referred to metallic or semiconductor material with their properties dependent on inner-atomic structure instead of on atoms composition themselves. A visible light rays can be bend by certain meta-materials and such behavior can also be noticed at infrared wavelengths.

The work on MPA design using Aperture coupling can be extended to:

- Using stacked MPAs, use of different value of dielectric constant and different material of substrate.

- Embedding different slot shapes on patch and ground.
- Use of impedance matching network for enhancement of the impedance bandwidth.

Feeding Techniques that can be used for future research:

Other than aperture coupled feed used in current research, various types of feeding techniques can also be used to design same MPAs like microstrip line feed, proximity coupled feed, coaxial probe feed and coplanar waveguide(CPW) feed for future work.

REFERENCES

[1] Rappaport T. *Wireless Communication: Principles and Practise*, 2nd edition, Pearson, (2009).

[2] Goldsmith A. *Wireless Communication,* Cambridge University Press., (2005).

[3] Siakavara K. and Nasimuddin N. *Microstrip Antennas*, Chapter-9, InTech. (2011)

[4] Mandelbrot B.B. *The Fractal Geometry of Nature,* San Francisco, CA: Freeman. (1983).

[5] Werner D.H. and Ganguly S. (2003). An overview of fractal antenna engineering research, *IEEE Antennas and Propagation Magazine*, 45(1), 38-57.

[6] Gianvittorio J.P. and Rahmat Y. (2002). Fractal antennas: A novel antenna miniaturization technique and applications, *IEEE Antenna and Propagation Magazine*, 44(1), 20-36.

[7] Balanis C.A. (1997). *Antenna Theory: Analysis and Design*, 2nd edition, United States of America, John Wiley & Sons Inc.

[8] Pozar D.M. and Duffy S.M. (1997). A dual-band circularly polarized aperture- coupled stacked microstrip antenna for global positioning satellite, *IEEE Transactions on Antenna and Propagation*, 45(11), 1618-1625.

[9] Kieda R. and Kitlinski M. (2004). Sierpinski monopole antenna - uniplanar feeding technique, *IEEE Microwaves, Radar and Wireless Communications*, 2, 477-480.

[10] Puente C., Romeu J., Pous R., Garcia X. and Benitez F. (1996). Fractal multiband antenna based on sierpinski gasket, *IEEE Electronics Letters*, 32, 1-2

[11] Puente C., Borau C., Rodero M.N. and Romeu J. (2002). An iterative model for fractal antennas: applications to the sierpinski gasket antenna, *IEEE Transactions on Antenna and Propagation*, 48(5), 713-719.

[12] Mishra R.K., Ghatak R., Poddar D.R. (2008). Design formula for sierpinski gasket pre fractal planar-monopole antennas, *IEEE Antennas and Propagation Magazine*, 50(3), 104-107.

[13] Yadav S., Choudhary R., Soni U., Peswani B. and Sharma M.M. (2014). Koch curve fractal antenna for Wi-MAX and C Band wireless applications, *IEEE International Conference on Confluence the Next Generation Information Technology Summit*, [5th: Noida, India: 2014], pp. 490-494.

[14] Vinoy K.J., Jose K.A., Varadan V.K. and Varadan V.V. (2001). Resonant frequency of hilbert curve fractal antennas, *IEEE Antennas and Propagation Society International Symposium*, 3, pp. 648-651.

[15] Aggarwal A. and Kartikeyan M.V. (2010). Pythagorean Tree: A fractal patch antenna for multi-frequency and ultra-wide bandwidth operations, *Progress in Electromagnetics Research*, 16, 25-35.

[16] Singh I., Tripathi V.S. (2011). Micro-strip patch antenna and its applications: A survey, *International Journal of Computer Technology and Applications*, 2, 1595-1599.

[17] Singh M., Basu A. and Koul S.K. (2006). Design of Aperture Coupled Fed Micro-Strip Patch Antenna for Wireless Communication," *IEEE India Conference*, [New Delhi, India: 2006], pp. 1-5.

[18] Werner D. H. (1995). An Overview of fractal electrodynamics research, *Annual Review of Progress in Applied Computational Electromagnetic*, 11, 964-969.

[19] Hohlfeld R.G. and Cohen N.. (1999). Self-Similarity and the geometric requirements for frequency independence in antenna, *Fractals*, 7(1), 79-84.

[20] Kaur M., Kaur A. and Khanna R. (2012). A microstrip patch antenna with aperture coupled technique 5.8 and 2 GHz. *MIT International Journal*, 2(2), 68-73.

[21] Kaur N. and Sivia J.S. (2016). Design of modified plus shape sierpinski carpet fractal antenna for S and C Band applications. *IEEE International Conference on Information Technology*, [Noida, India: 2016], pp. 230-235.

[22] Jagadeesha S., Vani R.M. and Hunugund P.V. (2012). Stacked plus shape fractal antenna for wireless application," *International Journal of Electronics And Communication Engineering & Technology*, 3(1), 286-292.

[23] Jagdeesha S., Vani R.M., Hunagund P.V. and Hegde P. (2013). Two element self-similar plus fractal antenna for wireless applications. *IEEE National Conference on Challenges in Research & Technology in Coming Decades*, [Ujire, India: 2013], pp. 1-5.

[24] Jibhkate N.S. and Zade P.L. (2016). A compact multiband plus shaped CPW fed fractal antenna for wireless applications, *IEEE International Conference on Green Engineering and Technologies*, [Coimbatore, India: 2016], pp. 1-5.

[25] Baliarda C. P., Romeu J.and Cardama A. (2000). The koch monopole: a small fractal antenna, *IEEE Transactions on Antennas and Propagation*, 11, 1773- 1781.

[26] Tang P. (2000). Scaling property of the koch fractal dipole, *IEEE International Symposium on Antennas and Propagation Digest*, 3, 150-153.

[27] Cohen N. (1997). Fractal antenna applications in wireless telecommunications, *Proceedings of the Electronics industries Forum of New England*, [Boston, MA, USA: 1997], pp. 43-49.

[28] El-Khamy S.E., Aboul-Dahab M.A. and Elkashlan M. (2000). A simplified koch multiband fractal array using windowing and quantization techniques," *IEEE International Symposium on Antennas and Propagation Digest*, 3, 1716-1719.

[29] Kim T., Yoo J. and Park H. (2001). The Koch island fractal microstrip patch antenna, *IEEE International Symposium on Antennas and Propagation Digest*, 2, 736-739.

[30] Sundaram A., Maddela M. and Ramadoss R. (2007). Koch-fractal folded-slot antenna charateristics, *IEEE Antenna and Wireless Propagation Letters*, 6, 219-222.

[31] Krishna D.D., Gopikrishna M., Anandan C. K., Mohanan P. and Vasudevan K. (2008). CPW-Fed koch fractal slot antenna for WLAN/WiMAX applications, *IEEE Transactions on Antennas and Propagarion Letters*, 7, 389-392.

[32] Puente C., Romeu1., Pous R. and Cardania A. (1998). On the behavior of the sierpinski multiband fractal antenna, *IEEE Transactions on Antennas and Propagation*, 46(4), 517-524.

[33] Choukiker Y.K. and Behera S.K. (2014). Modified sierpinski square fractal antenna covering ultra wideband applications with band notch characteristics, *Institution of Engineering And Technology, Microwave, Antenna Propagation*, 8(7), 506-512.

[34] Puente C., Romeu J., Bartoleme R. and Pous R. (1996). Perturbation of the sierpinski antenna to allocate operating bands, *IEEE Electronics Letters*, 32(24), 2186-2188.

[35] Puente C., Navarro M., Romeu J. and Pous R., "Variations on the fractal sierpinski antenna flare angle," *IEEE International Symposium on Antennas and Propagation Digest*, 4, 2340-2343.

[36] Song C. T. P., Hall P. S., Ghafouri-Shiraz H. and Wake D. (1999). Sierpinski monopole antenna with controlled band spacing and input impedance, *IEEElectronics Letters*, 35(13), 1036- 1037.

[37] Gonzalez J. M., Navano M., Puente C., Romeu I. and Aguasca A. (1999). Active zone self similarity of fractal-sierpinski antenna verified using infra-red thermo grams, *IEEElectronics Letters*, 35(17), 1393.1394.

[38] Kaur A. and Singh G. (2014). A review paper on fractal antenna engineering, *International Journal of Advance Resarch in Electrical, Electronics and Instrumentation engineering* , 3(6), 2320-3765.

[39] Kaur A., Khanna R. and Kartikeyan M.V. (2015). A stacked sierpinski gasket fractal antenna with a defected ground structure for UWB/WLAN/radio astronomy/Stm link applications, *Microwave and Optical Technology Letters*, 57(12), 2786-2792.

[40] Anguera J., Puente C., Borja C. and Montero R. (2001). Bowtie microstrip patch antenna based on the sierpinski fractal, *IEEE International Symposium on Antennas and Propagation Digest*, 3, 162-165.

[41] Parron J., Rius J.M. and Romeu I. (2001). Analysis of a sierpinski fractal patch antenna using the concept of macro basis functions," *IEEE International Symposium on Antennas and Propagation Digest*, 3, 616-619.

[42] Kaur A. (2015). Semi spiral G-shaped dual wideband microstrip antenna with aperture feeding for WLAN /WiMAX/U-NII band applications, *Signal Processing Symposium*, 8(6), 931-941.

[43] Kaur A., Khanna R. and Kartikeyena M.V. (2014). A stacked rectangular MSA with defected ground structure for IEEE 802.11b/g bands and WiMax applications. *International Conference on Microwave Antenna Propagation and Remote Sensing Engineering*. [Jodhpur, India: 2014], pp. 266–270.

[44] Bisht A. and Gupta M. (2016). A cup-shaped slotted microstrip patch antenna for UWB applications, *International Conference On Advance Computing, Communication & Automation,* [Dehradun, India: 2016], pp. 1-4.

[45] Azari A. (2011). A new super wideband fractal microstrip antenna, *IEEE Transactions On Antennas and Propagation*, 59(5), 1724-1727.

[46] Patil V.P. (2012). Enhancement of bandwidth of rectangular patch antenna using two square slots techniques, *International Journal of Engineering Sciences & Emerging Technologies*, 3(2), 1-12.

LIST OF PUBLICATIONS

PUBLISHED

- Kaur N. and Kaur A. (2017). Design of planar bowtie aperture coupled antenna for UWB applications, *International Conference on Advancements in Engineering and Technology*, [5th: Sangrur, India: 2017], pp. 92-94.
- Kaur N. and Kaur A. (2017). Design of a fractal aperture coupled microstrip antenna for UWB applications, *Journal of Microwave Engineering and Technologies*, 4(1), 19-22.

COMMUNICATED

- Kaur N. and Kaur A. (2017). A compact plus shaped carpet fractal antenna with an I-shaped DGS for C-band/X-band/UWB/WIBAN applications, *Wireless Personal Communication*.

Navneet_17.7.17

ORIGINALITY REPORT

%21	%10	%15	%9
SIMILARITY INDEX	INTERNET SOURCES	PUBLICATIONS	STUDENT PAPERS

PRIMARY SOURCES

1	Kaur, Amanpreet, Rajesh Khanna, and Machavaram V. Kartikeyan. "A stacked sierpinski gasket fractal antenna with a defected ground structure for UWB/WLAN/RADIO astronomy/STM Link applications", Microwave and Optical Technology Letters, 2015. Publication	%1
2	"Handbook of Antenna Technologies", Springer Nature, 2016 Publication	%1
3	Submitted to National Institute of Technology, Rourkela Student Paper	%1
4	ethesis.nitrkl.ac.in Internet Source	%1
5	Krishna, D.D., M. Gopikrishna, C.K. Aanandan, P. Mohanan, and K. Vasudevan. "Compact wideband Koch fractal printed slot antenna", IET Microwaves Antennas & Propagation, 2009. Publication	%1

6	Amanpreet Kaur. "Semi Spiral G-shaped dual wideband Microstrip Antenna with Aperture feeding for WLAN/WiMAX/U-NII band applications", International Journal of Microwave and Wireless Technologies, 2015 Publication	%1
7	Submitted to Punjab Technical University Student Paper	%1
8	ijarcsse.com Internet Source	%1
9	bradscholars.brad.ac.uk Internet Source	%1
10	Amanpreet Kaur, Rajesh Khanna. "Design and development of a stacked complementary microstrip antenna with a “π”-shaped DGS for UWB, UNII, WLAN, WiMAX, and Radio Astronomy wireless applications", International Journal of Microwave and Wireless Technologies, 2017 Publication	<%1
11	Submitted to Universiti Teknologi MARA Student Paper	<%1
12	Submitted to Higher Education Commission Pakistan Student Paper	<%1

13	Proceedings of the International Conference on Recent Cognizance in Wireless Communication & Image Processing, 2016. Publication	<%1
14	Dawit Fitsum, Dilip Mali, Mohammed Ismail. "Bandwidth Enhancement of Rectangular Microstrip Patch Antenna using Defected Ground Structure", Indonesian Journal of Electrical Engineering and Computer Science, 2016 Publication	<%1
15	eprints.utm.my Internet Source	<%1
16	Soren, Dipali, Rowdra Ghatak, Rabindra Kishore Mishra, and Dipak Ranjan Poddar. "Wideband Sierpinski Carpet Fractal Shaped Cylindrical Dielectric Resonator Antenna for X-Band Application", Journal of Electromagnetic Analysis and Application, 2012. Publication	<%1
17	cdn.intechopen.com Internet Source	<%1
18	Submitted to ABV-Indian Institute of Information Technology and Management Gwalior Student Paper	<%1

19	Submitted to Malaviya National Institute of Technology Student Paper	<%1
20	"Proceeding of International Conference on Intelligent Communication, Control and Devices", Springer Nature, 2017 Publication	<%1
21	www.jpier.org Internet Source	<%1
22	Lecture Notes in Electrical Engineering, 2015. Publication	<%1
23	Submitted to CSU, San Jose State University Student Paper	<%1
24	Submitted to University Tun Hussein Onn Malaysia Student Paper	<%1
25	Submitted to International Islamic University Malaysia Student Paper	<%1
26	Submitted to Indian Institute of Technology Jodhpur Student Paper	<%1
27	Submitted to University of Bradford Student Paper	<%1
28	Amanpreet Kaur, Rajesh Khanna, Machavaram	

	Kartikeyan. "A multilayer dual wideband circularly polarized microstrip antenna with DGS for WLAN/Bluetooth/ZigBee/Wi-Max/ IMT band applications", International Journal of Microwave and Wireless Technologies, 2015 Publication	<%1
29	V.V. Varadan. "Resonant frequency of Hilbert curve fractal antennas", IEEE Antennas and Propagation Society International Symposium 2001 Digest Held in conjunction with USNC/URSI National Radio Science Meeting (Cat No 01CH37229) APS-01, 2001 Publication	<%1
30	www.internationaljournalssrg.org Internet Source	<%1
31	Submitted to University Der Es Salaam Student Paper	<%1
32	etd.adm.unipi.it Internet Source	<%1
33	Mandeep Kaur, Jagtar Singh Sivia. "On the Design of Plus Slotted Fractal Antenna Array", Open Journal of Antennas and Propagation, 2016 Publication	<%1
34	Submitted to Madan Mohan Malaviya University of Technology Student Paper	<%1

35	Submitted to Thapar University, Patiala Student Paper	<%1
36	Basu, . "Z", Dictionary of Geophysics Astrophysics and Astronomy, 2001. Publication	<%1
37	Islam, Md., Mohammad Islam, Mohammad Faruque, Md. Samsuzzaman, Norbahiah Misran, and Haslina Arshad. "Microwave Imaging Sensor Using Compact Metamaterial UWB Antenna with a High Correlation Factor", Materials, 2015. Publication	<%1
38	Palandöken, Merih. "Microwave Metamaterials for Compact Filters and Antennas", Technische Universität Berlin, 2012. Publication	<%1
39	Tomar, Sanjiv, and Ajay Kumar. "Design of a novel compact planar monopole UWB antenna with triple band-notched characteristics", 2015 2nd International Conference on Signal Processing and Integrated Networks (SPIN), 2015. Publication	<%1
40	old.oalib.com Internet Source	<%1
41	Submitted to Universiti Malaysia Perlis	

Student Paper

<%1

42	Jeemon, Basil K, K Shambavi, and Zachariah C Alex. "A multi-fractal antenna for WLAN and WiMAX application", 2013 IEEE CONFERENCE ON INFORMATION AND COMMUNICATION TECHNOLOGIES, 2013. Publication	<%1
43	file.scirp.org Internet Source	<%1
44	Submitted to iGroup Student Paper	<%1
45	Submitted to University of Liverpool Student Paper	<%1
46	Pal, A., A. Mehta, D. Mirshekar-Syahkal, and H. Nakano. "Semi doughnut pattern Square Loop Antenna for vehicular and wireless applications", 2011 IEEE International Symposium on Antennas and Propagation (APSURSI), 2011. Publication	<%1
47	Yadav, Sanjeev, Ruchika Choudhary, Umesh Soni, Bhavana Peswani, and Mahendra Mohan Sharma. "Koch curve fractal antenna for Wi-MAX and C-Band wireless applications", 2014 5th International Conference - Confluence The	<%1

Next Generation Information Technology Summit (Confluence), 2014.
Publication

---

48 Singhal, Sarthak, and Amit Kumar Singh. "Crescent-shaped dipole antenna for ultrawideband applications", Microwave and Optical Technology Letters, 2015. <%1
Publication

---

49 Kohli, Saurabh, Sukhwinder Singh Dhillon, and Anupama Marwaha. "Design and Optimization of Multiband Fractal Microstrip Patch Antenna for Wireless Applications", 2013 5th International Conference on Computational Intelligence and Communication Networks, 2013. <%1
Publication

---

50 Hegde, S.P., S. Jagadeesha, P.V. Hunagund, and R.M. Vani. "Two element self-similar plus shape fractal antenna for wireless applications", National Conference on Challenges in Research & Technology in the Coming Decades (CRT 2013), 2013. <%1
Publication

---

51 Submitted to Indian Institute of Technology-Bhubaneswar <%1
Student Paper

---

52 Submitted to Gulf University

	Student Paper	<%1
53	www.ijritcc.org Internet Source	<%1
54	dyuthi.cusat.ac.in Internet Source	<%1
55	www.slideshare.net Internet Source	<%1
56	Lee, Sung-woo, and Youngje Sung. "Compact Frequency Reconfigurable Antenna for LTE/WWAN Mobile Handset Applications", IEEE Transactions on Antennas and Propagation, 2015. Publication	<%1
57	blog.engglib.upd.edu.ph Internet Source	<%1
58	earsiv.cankaya.edu.tr:8080 Internet Source	<%1
59	Submitted to Guru Nanak Dev Engineering College Student Paper	<%1
60	COMPEL: The International Journal for Computation and Mathematics in Electrical and Electronic Engineering, Volume 31, Issue 6 (2012-11-10)	<%1

	Publication	
61	Springer Series in Optical Sciences, 2014. Publication	<%1
62	Gundeti, Praveen, M. Sreenivasan, K. George Thomas, P. Ezhilarasi, and A. Ayshathul Fouzia. "A frequency reconfigurable wide slot antenna", 2013 IEEE Applied Electromagnetics Conference (AEMC), 2013. Publication	<%1
63	Qi Wu. "", IEEE Transactions on Antennas and Propagation, 3/2008 Publication	<%1
64	inpressco.com Internet Source	<%1
65	Submitted to Segi University College Student Paper	<%1
66	Submitted to Visvesvaraya Technological University Student Paper	<%1
67	www.rroij.com Internet Source	<%1
68	Submitted to University of Nottingham Student Paper	<%1
69	Advances in Intelligent Systems and Computing, 2016.	<%1

	Publication	
70	Sim, Chow-Yen-Desmond, Yi-Wen Hsu, and Guanli Yang. "Slits Loaded Circularly Polarized Universal UHF RFID Reader Antenna", IEEE Antennas and Wireless Propagation Letters, 2015. Publication	<%1
71	Submitted to Panjab University Student Paper	<%1
72	linknovate.com Internet Source	<%1
73	"Book alert", Proceedings of the IEEE, 1982 Publication	<%1
74	Submitted to Charotar University of Science And Technology Student Paper	<%1
75	Submitted to ICFAI University Student Paper	<%1
76	Singhal, Sarthak, Tushar Goel, and Amit Kumar Singh. "HEXAGONAL TREE SHAPED ULTRA WIDEBAND FRACTAL ANTENNA", International Journal of Electronics Letters, 2016. Publication	<%1
77	researchrepository.napier.ac.uk Internet Source	<%1

78	Submitted to Brunel University Student Paper	<%1
79	ijrte.academypublisher.com Internet Source	<%1
80	Najafpour, Mahdi, Negin Manshouri, Ayhan Yazgan, and Masoud Maleki. "A novel semicircular fractal antenna design with single band-notch property for ultra wide band systems", 2015 38th International Conference on Telecommunications and Signal Processing (TSP), 2015. Publication	<%1
81	Taheri, Mohammad Mehdi Samadi, Hamid R. Hassani, and Sajad Mohammad Ali Nezhad. "Compact printed coplanar waveguide-fed ultra-wideband antenna with multiple notched bands", Microwave and Optical Technology Letters, 2012. Publication	<%1
82	Visser. "PCB Antennas: Printed Monopoles", Approximate Antenna Analysis for CAD, 03/13/2009 Publication	<%1
83	Susila M, , and T Rama Rao. "Design of a novel microstrip-fed UWB fractal antenna for Wireless Personal Area communications", 2015	<%1

	International Conference on Advances in Computing Communications and Informatics (ICACCI), 2015. Publication	
84	digital-library.theiet.org Internet Source	<%1
85	Kumar, Yadwinder, and Surinder Singh. "A Compact Multiband Hybrid Fractal Antenna for Multistandard Mobile Wireless Applications", Wireless Personal Communications, 2015. Publication	<%1
86	"Antenna Theory - Analysis and Design.", Microwave Journal, May 1998 Issue Publication	<%1
87	docplayer.net Internet Source	<%1
88	Submitted to Universiti Teknikal Malaysia Melaka Student Paper	<%1
89	www.ijcaonline.org Internet Source	<%1
90	eprints.soton.ac.uk Internet Source	<%1
91	www.dtic.mil Internet Source	<%1

92	Barroso, R., and M. Diaz. "Side notched two-stage Parany monopole antenna", Proceedings of the 2012 IEEE International Symposium on Antennas and Propagation, 2012. Publication	<%1
93	Hansen. "Electrically Small Antennas", Electrically Small Superdirective and Superconducting Antennas, 07/07/2006 Publication	<%1
94	Abraham, Jacob, and Thomaskutty Mathew. "David fractal antenna for multiband wireless communication", 2014 2nd International Conference on Electronic Design (ICED), 2014. Publication	<%1

EXCLUDE QUOTES	ON	EXCLUDE MATCHES	< 10 WORDS
EXCLUDE BIBLIOGRAPHY	ON		